Journal of Environmental Management 303 (2022) 114122

Contents lists available at ScienceDirect

Journal of Environmental Management

journal homepage: www.elsevier.com/locate/jenvman

Tributary effects on the ecological responses of a regulated river to experimental floods

Gabriele Consoli [a,b,*], Rudolf M. Haller [c], Michael Doering [d,e], Saman Hashemi [f], Christopher T. Robinson [a,b]

[a] Department of Aquatic Ecology, Eawag, 8600, Dübendorf, Switzerland
[b] Institute of Integrative Biology, ETH-Zürich, 8092, Zürich, Switzerland
[c] Swiss National Park, Chastè, Planta-Wildenberg, 7530, Zernez, Switzerland
[d] Institute of Natural Resource Sciences, Zurich University of Applied Sciences (ZHAW), Wädenswil, Switzerland
[e] eQcharta GmbH, Wädenswil, Switzerland
[f] Department of Geography, University of Leeds, UK

ARTICLE INFO

Keywords:
Environmental flows
Metabolism
Disturbance
Macroinvertebrates
Geomorphology

ABSTRACT

Rivers regulated by dams display several ecosystem alterations due to modified flow and sediment regimes. Downstream from a dam, ecosystem degradation occurs because of reduced disturbance, mostly derived from limitations on flow variability and sediment supply. In the last decade, most flow restoration/dam impact mitigation was oriented towards the development of environmental flows. Flow variability (and consequent disturbance) can be reintroduced by releasing artificial high flows (experimental floods). Flow-sediment interactions during experimental floods represent strong ecosystem drivers, influencing nutrient dynamics, and metabolic and functional properties. In river networks, sediment and water inputs from tributaries generate points of discontinuity that can drive major changes in environmental conditions, affecting habitat structure and determining functional differences between upstream and downstream. However, despite the relevance for management, flow/sediment relations during environmental flows – and more importantly during experimental floods – remain poorly understood, mostly due to the lack of empirical evidence. In this study, we examined how a major tributary (source of water and sediments) modified the physical habitat template of a regulated river, thereby influencing ecological and geomorphological responses to experimental floods. Methods combined high-resolution drone mapping techniques with a wide range of biological samples collected in field surveys before, during, and after experimental floods in an alpine river. Data were used to quantify changes in relevant functional and structural ecosystem properties, relating ecological responses to geomorphological dynamics. Results highlight the importance of tributaries in restoring ecosystem properties lost after damming, enhancing the resilience of the system. In addition, we observed that disturbance legacy played a fundamental role in determining ecological conditions of a river prior to experimental floods, thus confirming that considering flow variability and sediment availability is crucial in adaptive dam management and environmental flows design.

1. Introduction

A rivers' natural flow regime is characterized by fluctuations in discharge between low flows/droughts and high flows/floods, tightly coupled with precipitation/snowmelt events, generally with some degree of seasonal predictability (Poff et al., 1997). Rivers also have a natural sediment regime, which depends on the geological configuration and topography of the catchment (Wohl et al., 2015). Floods are among the main sources of natural disturbance in streams (Lake, 2000) and function as an important connection between flow and sediment regimes, controlling stream geomorphological dynamics and ensuring lateral connectivity with adjacent floodplains. The erosional forces by flow and sediment during a flood play a key role in sustaining the natural heterogeneity of fluvial habitat mosaics (Stanford et al., 2005), determining the spatial and temporal variation in the distribution of nutrients, organic resources, and habitat suitability for stream organisms, thereby influencing all trophic levels of aquatic food webs (Robinson et al., 2002). During floods, organic matter and biota are

* Corresponding author. Department of Aquatic Ecology, Eawag, 8600, Dübendorf, Switzerland.
E-mail address: gabriele.consoli@eawag.ch (G. Consoli).

https://doi.org/10.1016/j.jenvman.2021.114122
Received 15 June 2021; Received in revised form 8 October 2021; Accepted 14 November 2021
Available online 25 November 2021

transported and redistributed along the river network (Golladay et al., 1987; Small et al., 2008). Specific life-history traits allow stream and terrestrial organisms to benefit from floods – and low flow windows between floods (Lytle and Poff, 2004; Poiani, 2006), as well as providing resistance and resilience to extreme events (e.g., Robinson, 2012). Many aquatic organisms rely on floods for reproductive or dispersal cues (e.g., Jiménez-Segura et al., 2010), and fish spawning and fry-rearing habitats are in many cases dependent on the seasonal pulse of floods (Chapman, 1988; Junk et al., 1989; Melis, 2011).

Nowadays, many rivers are heavily regulated, modifying natural flow and sediment regimes. River regulation contributes greatly to the global crisis of freshwater ecosystems (Dudgeon et al., 2006; Reid et al., 2019), where severe hydropower-related morphological and hydrological modifications add to stressors related to other human activities (Malmqvist and Rundle, 2002). The scale of this alteration is testified by the proliferation of studies on the effects of river regulation at a global level (e.g., Maavara et al., 2020; Turgeon et al., 2019; Vörösmarty et al., 2003). The rush towards sustainable energy production, coupled with future uncertainty in water security due to climate change, has strongly increased the strategic function of dams (Vörösmarty et al., 2010).

The number of large dams constructed is increasing, now over 55,000 worldwide, especially in developing countries (Winemiller et al., 2016; Zarfl et al., 2015), and only slightly compensated by removal of old and obsolete structures (O'Connor et al., 2015). The main alterations of the hydrological regime and sediment regime caused by dams are a reduction in flow variability and water availability, and sediment supply (Poff et al., 1997). Modified flow and sediment regimes alter the physical habitat template of a river downstream of a dam (Ward and Stanford, 1983). For instance, the combined effect of disruption in flow variability and sediment transport reduces flow-generated disturbance, increases streambed stabilization and promotes channel incision, resulting in physical habitat degradation. As a response to new habitat conditions, the biotic properties of a river undergo major structural and functional adjustments (Bunn and Arthington, 2002). For instance, flow/sediment regulation influences rates of downstream metabolic processes (Aristi et al., 2014) and resource availability (e.g., increased algal growth, Lessard et al., 2013). Further, native riparian and aquatic organisms are affected during important life stages, thus species preferring stable conditions become dominant, and invasion by alien species is facilitated (Bunn and Arthington, 2002).

There is growing awareness of the importance of interactions and relationships between hydrological, geomorphological, and ecological processes (Grabowski and Gurnell, 2016) to face the profound environmental modification and ecological consequences of river regulation (Poff, 2018). In adaptive dam management, environmental flows aim at targeting functional components of the natural flow regime (i.e., functional flows after Yarnell et al., 2015) link flow dynamics to ecosystem processes. Flow experiments (Konrad et al., 2011; Olden et al., 2014) or managed environmental flows (Gillespie et al., 2015) have been increasingly designed and implemented to modify dam water-release schemes to restore river geomorphology and ecological properties. For example, stable residual flows from dams can be mitigated by the implementation of experimental floods, which are outflow manipulations aimed at reintroducing elements of flow variability in regulated rivers (Robinson et al., 2018). Experimental floods can be used as management actions to enhance geomorphological/ecological conditions below dams and serve as large-scale flow experiments to improve the understanding of geomorphological/ecological response mechanisms to such disturbances (Konrad et al., 2011). Prime examples of long-term experimental flood applications are those of the Colorado (Cross et al., 2011) and Spöl River (Robinson et al., 2018). These studies provide a foundation on the topic, showing that ecosystem responses to extreme flow manipulations depend on the time-frame, status of abiotic components, and the adaptation of organisms to flood disturbance.

Tributaries can have important roles in determining different upstream/downstream responses to flow experiments (Vinson, 2001). In fact, unregulated tributaries are points of discontinuity that can generate major changes in the environmental conditions of a river (Vannote et al., 1980), and can revert or mitigate some of the impacts of flow regulation (Milner et al., 2019; Ward and Stanford, 1983). Tributaries can introduce substantial amounts of water, sediments, and organic matter that partially restore flow variability, and function as recruitment sources of stream organisms (Rice et al., 2001; Rice et al., 2006). Sediment and water inputs from tributaries can modify key aspects of the physical template of streams, determining changes in bottom hydraulics and substrate stability, thus generating an ideal environmental gradient to study flow-sediment-ecology relationships and responses to experimental floods.

The identification of specific patterns of eco-morphological response at different time resolutions (e.g., immediate, short term, long term) to flow manipulation is essential for water managers to generate explicit endpoints for an ecologically sound flow/sediment restoration (Harrison et al., 2017; Kiernan et al., 2012; Robinson et al., 2004a, 2018; Thompson et al., 2018). The understanding of mechanistic relationships between flow restoration and environmental/ecological responses is still insufficient to link restoration methods and goals. Environmental flow planning needs to be objective-driven (Davies et al., 2012) as outcomes are likely to be context-dependent (Gillespie et al., 2015; Kevic et al., 2018; Olden et al., 2014). Further, the need to understand how sediment availability influences ecological and morphological responses to flow manipulations is motivated by a risk of unsuccessful or even deleterious flow restorations if evaluations on sediments are neglected (Wohl et al., 2015).

Our study aimed at measuring ecological and morphological responses to experimental floods in a regulated river, as influenced by an unregulated tributary. We compared ecosystem baseline, response, and recovery properties after two experimental floods above and below a tributary input, and assessed the immediate ecological response patterns during each flood. We expected the two reaches to respond differently, and to relate the differences to disturbance frequency and sediment supply. We hypothesized that ecological components below the tributary will show attributes of resistance and resilience to floods disturbance. Our ultimate goal was to improve the understanding of ecosystem responses and eco-morphological relationships during experimental floods and to highlight the importance of periodic disturbance in maintaining the ecological properties of regulated rivers.

2. Methods

2.1. Study site

The Spöl catchment (295 km^2) is located in the central Alps as part of the Danube basin (Fig. 1). Some ~80% of the catchment lies in Stelvio National Park, Italy, and the Swiss National Park (SNP), Switzerland. The Spöl is 28-km long, originating from Forcola di Livigno at 2315 m above sea level, flows into the Inn River at Zernez, Switzerland. From 1960 to 1970, Punt dal Gall (164M m^3 reservoir capacity) and Ova Spin (6.2M m^3 reservoir capacity) dams were built along its course for energy production (Scheurer and Molinari, 2003). Before regulation, the Spöl had a glacio-nival regime with winter low flows and higher flows during the other seasons, including floods generated by rainfall events (see hydrological data presented in Robinson et al., 2018). Due to the eco-morphological impacts caused by the dams, a board composed of members of the Swiss National Park, the hydropower company Engadiner Kraftwerke (EKW), Federal and Cantonal authorities agreed to an experimental flood program starting in 2000. The flood program aimed to reduce colmation, increase substrate porosity by reducing periphyton levels and flushing fine sediments from the riverbed, and restoring channel morphology. Since 2000, floods have been implemented regularly once or twice each year, with controlled water releases from Ova Spin and Punt dal Gall (Kevic et al., 2018; Robinson et al., 2018). This study was carried out on the lower segment of the river, from

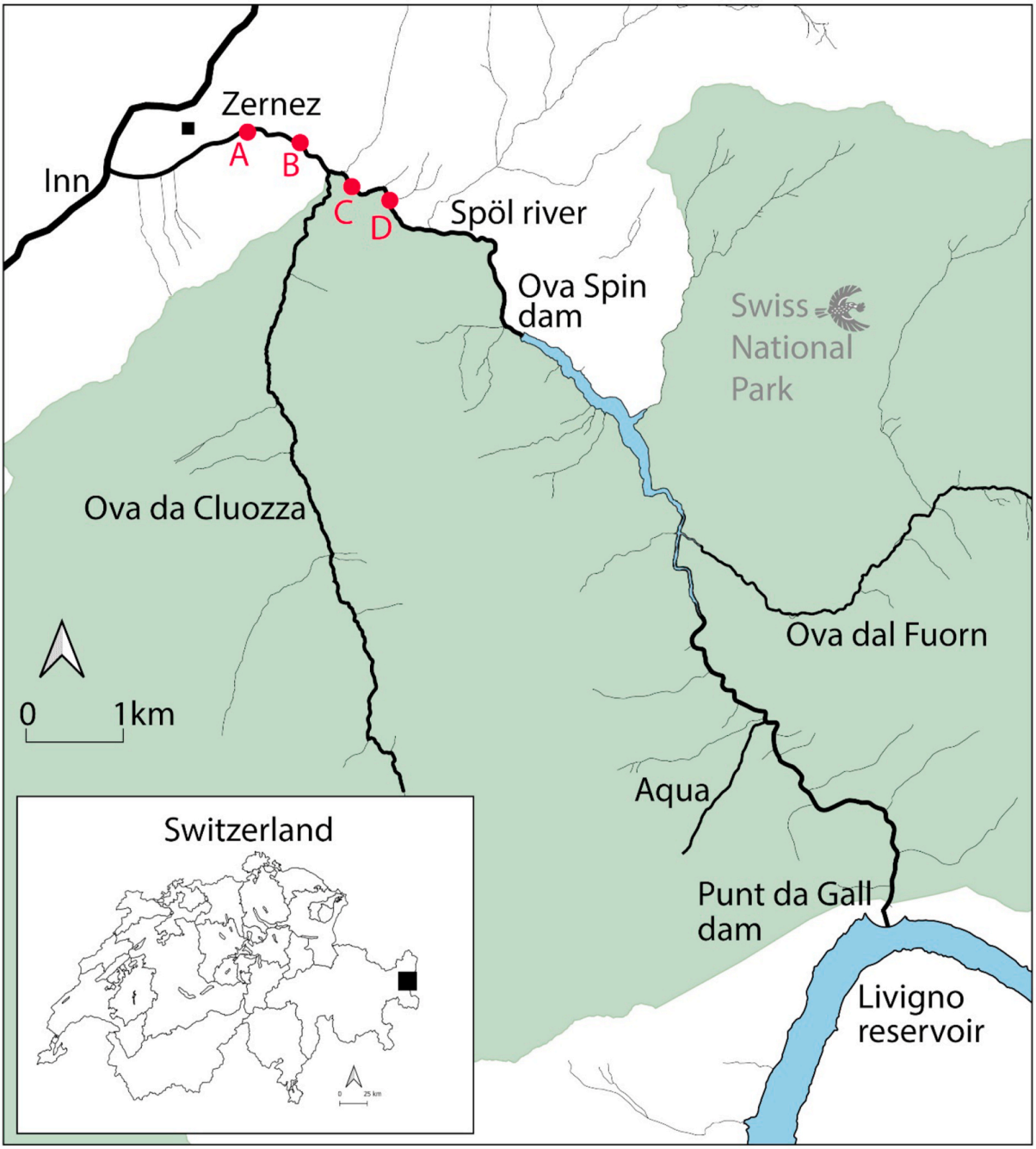

Fig. 1. Study area and location of reservoir dams (Punt da Gall, Ova Spin). A-D indicate the location of sites for before/after and during each flood sample collection. A, B are located below the junction with the tributary (Ova da Cluozza); C, D are located above. Site D and site A mark the boundaries of the drone flights.

Ova Spin dam to the junction with the River Inn (Fig. 1).

The tributary, Ova da Cluozza, is a left bank unregulated tributary of the lower Spöl with a catchment of 27 km^2 (Fig. 1). Its flow regime is characterized by marked seasonality of winter low flows and frequent summer spates (Fig. 2). During baseflow, it adds 0.2–0.8 m^3/s to the Spöl discharge (~0.4 m^3/s winter residual flow; ~0.9 m^3/s summer residual flow), while during periods of snowmelt and rainfall, it generates floods of 4–8 m^3/s (see Fig. 2) and adds substantial inputs of sediment. This offers the opportunity to study how sediment dynamics vary and how ecological resistance and resilience to experimental floods differ on the river Spöl above and below the confluence. The two reaches (upstream and downstream of the confluence) have comparable water physico-chemical conditions but are different in morphology, streambed structure, and to some extent substrate composition (Mathers et al., 2021). The upper 3.5-km long section flows between Ova Spin dam and the junction with Ova da Cluozza through a mainly confined valley. Trees (mostly *Pinus* sp.) cover the steep banks, and many side scree slopes are present along the reach. A small tributary (Ova da Lasciadura) enters at around halfway in the upper reach. The study reach is characterized mostly by a single thread channel with riffles, pools, and small glides. The lower section is ~2.5-km long and flows from the junction with Ova da Cluozza to the Inn. Riparian vegetation is composed of trees (mostly *Pinus* sp. and *Alnus* sp.) and pasture near the town of Zernez. This section flows through an open valley, with vegetated islands and long bars, where the channel often braids forming riffles and glides.

Two experimental floods were released (September 4, 2018, July 19,

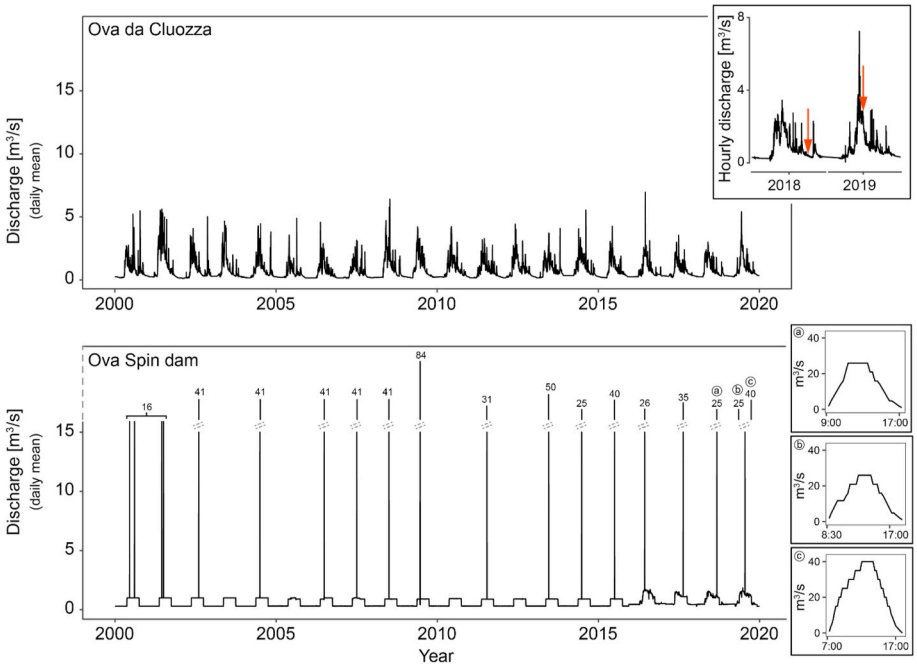

Fig. 2. Historical daily mean discharge from Ova da Cluozza (upper panel) and Ova Spin (lower panel). The inset in the Ova da Cluozza panel shows a detail of the Ova da Cluozza discharge conditions in 2018 and 2019 (hourly measurements). The arrows in the inset indicate the moment at which the experimental floods (2018 and first one of 2019) were released. In the Ova Spin panel, the water release pattern (~0.4 m^3/s winter residual flow; ~0.9 m^3/s summer residual flow) and the experimental floods implemented since 2000 are shown. The numbers on the flood peaks indicate the highest discharge reached. The insets in the Ova Spin panel show the hydrographs of the floods presented in this study. Data source: FOEN – Federal Office for the Environment (Ova da Cluozza); EKW (Ova Spin). Location of gauging stations: Ova da Cluozza 46°41′35.37″N 10°07′06.09″E; Ova Spin 46°40′42.16″N 10°08′38.66″E.

2019) from Ova Spin dam from the outlet located at the bottom of the dam (Scheurer and Molinari, 2003). Duration of both floods was ~8 h with a maximum discharge of 25 m^3/s maintained for ~2 h. Volumes of water released during the floods were 4.6 × 10^5 m^3 (2018) and 5.1 × 10^5 m^3 (2019). Peak discharges were in the typical range of seasonal high flows in the system before impoundment for autumn rainfalls (Sept. 2018) and snowmelt (July 2019) (Robinson and Uehlinger, 2008). The floods had similar magnitude but different release patterns, with the 2018 flood characterized by a steeper rising limb and shorter duration (see hydrographs in Fig. 2). Samples were collected before (BF), during, after (AF), and four weeks after each flood (LAF) to observe patterns of response of a series of ecological parameters. BF, AF, LAF sampling was carried out at four locations, two above (C, D) and two below (A, B) the junction with the tributary (Fig. 1). Sampling during the floods was carried out at two locations, one above (D) and one below (A) the confluence. In 2019, three days after the study flood, EKW, and SNP decided to release another flood of greater magnitude (40 m^3/s, 10.4 × 10^5 m^3). This flood was not sampled as the very short notice made organizing sampling practically impossible. Analyses and plotting were carried out using R 3.6.0 (R Core Team, 2019). Historical hydrological data (2000–2019) from Ova da Cluozza and Ova Spin, as well as the flood hydrographs, are presented in Fig. 2.

2.2. Sampling during each flood

2.2.1. Physico-chemical monitoring

Water temperature, electrical conductivity (μS cm^{-1} at 20 °C) (WTW LF340, Wielheim, Germany) and turbidity (Hach Lange TSS portable) were recorded, and a 0.5 l water sample was collected at defined time intervals during each flood; every ~15 min during the rising limb of the hydrograph and every ~30 min after. Sampling also included one baseline sample taken before and the day after the 2018 flood, and one baseline sample before, two (morning and afternoon) after the 2019 flood, and one sample taken four weeks later. Water samples were refrigerated during transport to the laboratory and then analyzed for total nitrogen (TN), and total phosphorus (TP). The first four water samples of the 2019 flood from site A are not included due to technical issues.

2.2.2. Seston and drift samples

Seston/drift samples were collected with a handheld driftnet with a rectangular opening (0.1 × 0.3 m; 400μ mesh) at the same temporal scheme as for physico-chemical samples. Each sample was collected for a defined amount of time, varying between 10 and 180s, depending on the clogging of the net. Water velocity was measured at the mouth of the net (MiniAir2, Schiltknecht AG, Gossau, Switzerland) to calculate the volume of water filtered. Only samples collected at the most upstream (D) and most downstream (A) sites were analyzed. In total, 21 samples were collected at each sampling site in 2018 and, respectively, 25 (site A) and 21 (site D) in 2019. In addition, two drift samples were collected at both sites the day after (morning/afternoon) and one four weeks after the second flood.

Seston/drift samples were stored in plastic bags and frozen at −20 °C until analysis. In the laboratory, macroinvertebrates were separated from organic matter using a dissecting microscope (10X) and preserved in 70% ethanol. Some large samples were subsampled by half or a quarter before sorting. Macroinvertebrates were identified to the lowest practical taxonomic level (mostly genus) using Tachet et al. (2010). Large pieces of wood were separated from the remaining organic matter before analysis of dry mass. Organic matter content was obtained by measuring ash-free dry mass (AFDM) by drying at 60 °C for 48h, incinerating at 500 °C for 5 h, and then recording the difference in weights. To quantify transport during the flood, the number of invertebrates transported, and organic matter biomass were standardized for the water volume filtered for each sample and expressed, respectively, as gAFDM/m^3 and N/m^3.

2.2.3. Data analysis

Transported organic matter and invertebrates (seston/drift), as well as physico-chemistry data, were synchronized to modeled discharge data to allow for an exact representation of temporal patterns in respect to each flood. Numerical modeling was used to simulate the discharge during each experimental flood. The Delft3D-FLOW module was employed to set up the model and execute the flow simulation (Saman Hashemi unpublished data). We calculated total organic matter biomass and macroinvertebrate drift based on water volume release data obtained from EKW. We tracked the response of taxa with behavioral traits relevant to flood disturbance by looking at single flood response patterns

of Baetidae (active swimmers), Heptagenidae and Rhyacophilidae (clingers), Chironomidae (passive), Gammaridae (swimmer/passive), and Nemouridae (crawler/passive). Their relative abundances were plotted against discharge to identify trait patterns in functional response to floods.

2.2.4. Data deposition

Physicho-chemical, seston, and drift data available on request from Zenodo (Consoli et al., 2021).

2.3. Measures collected before/after each flood

2.3.1. Benthic samples and sediment respiration

Quantitative benthic samples of organic matter and macroinvertebrates were collected at three random points at each site on each sampling date using a Hess sampler (sampling surface of 0.045 m^2, 250μ mesh), and stored in 70% ethanol. Macroinvertebrates were sorted from organic matter and identified as above. Organic matter was separated into coarse and fine particulate organic matter (FPOM < 1 mm < CPOM) and analyzed as ash-free dry mass (g/m^2).

Five stones were collected at each site on each sampling date for measuring periphyton biomass and frozen at −20 °C until analysis. Measurements of the two main axes (a-, b-axis) were taken for each stone to calculate the surface sampled using the equation a*b*π/4. Periphyton was scraped from the stone surface using a metal brush and rinsed with water. The sample volume was recorded, and a subsample was filtered through a glass fiber filter (Whatman GF/F). Filters were dried at 60 °C, weighed, ashed at 500 °C for 3 h, and reweighed to estimate periphyton biomass as AFDM ($gAFDM/m^2$).

Hyporheic sediment respiration was measured before and after each flood to evaluate microbial responses to flooding. In situ respiration chambers were used to measure oxygen depletion after Uehlinger et al. (2002). Four replicates per location were used to carry out the experiment. The upper layer of sediment (~10 cm) was removed before sample collection to exclude the effect of primary producers on respiration. Sediments were sieved with an 8-mm sieve to standardize measures following Uehlinger et al. (2003). Plexiglas® tubes (678 cm^3) were half-filled with sediments, then filled with stream water and sealed. Tubes were incubated in darkness for at least 4 h in the stream channel at each site. Dissolved oxygen content and temperature were measured before and after incubation with a dissolved oxygen meter (Hach HQ40d equipped with LD0101 oxygen probe). After measurement, the content of each tube was stored in plastic bags and kept at −20 °C until analyzed for sediment volume, grain size distribution, and loose (LPOM, expressed as gAFDM/l) and attached particulate organic matter (APOM, expressed as $g/kg_{(sed.<8mm)}$). Oxygen depletion was standardized for temperature, sediment weight, and organic matter content.

2.3.2. Data analysis

Results from sediment respiration, periphyton, CPOM, FPOM, and macroinvertebrate density from benthic samples were grouped relative to their location (A, B downstream; C, D upstream), and the mean and standard error then calculated. A two-way ANOVA was used to test individual responses to experimental floods between upstream and downstream sites (factors: reach, sampling date, and sampling date × reach) on (log+1) transformed data to meet assumptions. Of interest for this study were reach and the interaction between sampling date and reach. In the case of significant results (alpha = 0.05), Tukey's HSD test was used to identify significant differences.

2.3.3. Drone surveys

Drone surveys were flown over the study segment (Fig. 1) before and after each flood, under baseflow conditions, to collect data (images) to assess morphological changes following the floods. A Wingtra One drone equipped with a high-resolution RGB camera (Sony RX1; 42 MP) and an Intel® Falcon™ 8 with a high-resolution RGB camera (Sony NEX-7; 24.3 MP) were used, respectively, in 2018 and 2019. Ground control points measured with a dGPS (n = 10 in 2018; n = 50 in 2019) were used to reach high accuracies in the rectification of the ortho-images. Generation of orthophotos was done with the Software Pix4D. The software relied on automatic feature detection and matching algorithms to retrieve the internal and external orientation of oblique images. Photogrammetric processing subsequently provided dense point clouds, digital elevation models (DEM), and ortho-images. The resolution of ortho-images was < 3 cm.

Large-scale morphological responses to each flood were tracked on the aerial images in QGIS 3.10.2 by separating the following macro-unit surfaces within the bankfull area: emerged sediment, wet channel, and instream vegetation (Geomorphic Units Survey (GUS) – broad level, Belletti et al., 2017). Polygons were hand-drawn in a vector layer to extract the area of each macro-unit type to estimate changes in mean size, variance, and relative abundance before and after a flood. Macro-units were identified at a scale of 1:250, and a scale of 1:125 was used in cases of difficult or ambiguous interpretation. Four maps (Fig. S1 in supplementary material) were generated as follows: before 2018 flood, after 2018 flood, after 2019 first flood, after 2019 s flood. Reach length was of ~800 m upstream and ~1500 m downstream. Based on these results, ratios between wet/dry surfaces were calculated for each map, and comparisons between reaches were carried out by adjusting macro-units surfaces to reach length (upstream/downstream).

Reach-scale changes in geomorphic units assemblage over the study period were assessed by applying the GUS method to the basic level. In this case, three sub-reaches of interest of ~500 m were identified, one upstream and two downstream of the confluence (mid and lower); see Fig. S1 in supplementary material for the location of the sub-reaches. Polygons were hand-drawn on a vector layer to extract the area of each geomorphic unit and sub-unit types relevant to the habitat level, to estimate changes in relative abundance of each geomorphic unit after the three floods (i.e., before 2018 flood and after the second 2019 flood). The following geomorphic units and sub-units were identified at a scale of 1:125, zooming in when necessary: rapid, riffle, pool/backwater, glide, deposition of boulders/cobbles (S – partially submerged, E – emerged), mid channel bar, bank attached bar, vegetated bar, vegetated island (shrubs and trees), trees in active channel. Two sets of maps were generated as follows: before 2018 flood, after 2019 s flood (Fig. 7). To estimate changes in channel width, measurements were taken every 5 m, perpendicular to a centerline with the Geometric Attributes tool (Nyberg et al., 2015) in QGIS 3.10.2, and mean and standard deviation were calculated. For each sub-reach wet/dry surface changes of the active channel were calculated based on geomorphic units areas. Change in surface occupied from each unit was calculated as the difference between maps and shown in Fig. 7.

3. Results

3.1. Immediate responses to the floods

3.1.1. Physico-chemical responses during the floods

Patterns of temperature, conductivity, total nitrogen, and total phosphorus showed minimal differences between upstream and downstream sites, but notable differences between floods (Fig. 3). During the 2018 flood, changes in temperature were in the range of ~1.5 °C. Water baseline temperature was ~8 °C at both reaches. Temperature increased by ~0.5 °C (upstream) and 1.0 °C (downstream) during the early phases of the flood, likely due to the presence of cooler water layers inside the reservoir. Upstream, temperature stabilized around 8.3 °C and slowly increased to 9 °C during the falling limb. Downstream, water temperature remained stable at around 9 °C during the flood, with slight oscillations of ±0.3 °C. During the 2019 floods, the patterns of response were comparable between reaches, (downstream temperatures shifted −1 °C due to the input of cooler water from the tributary), and showed a gradual increase in temperature consistent with the daily solar heating,

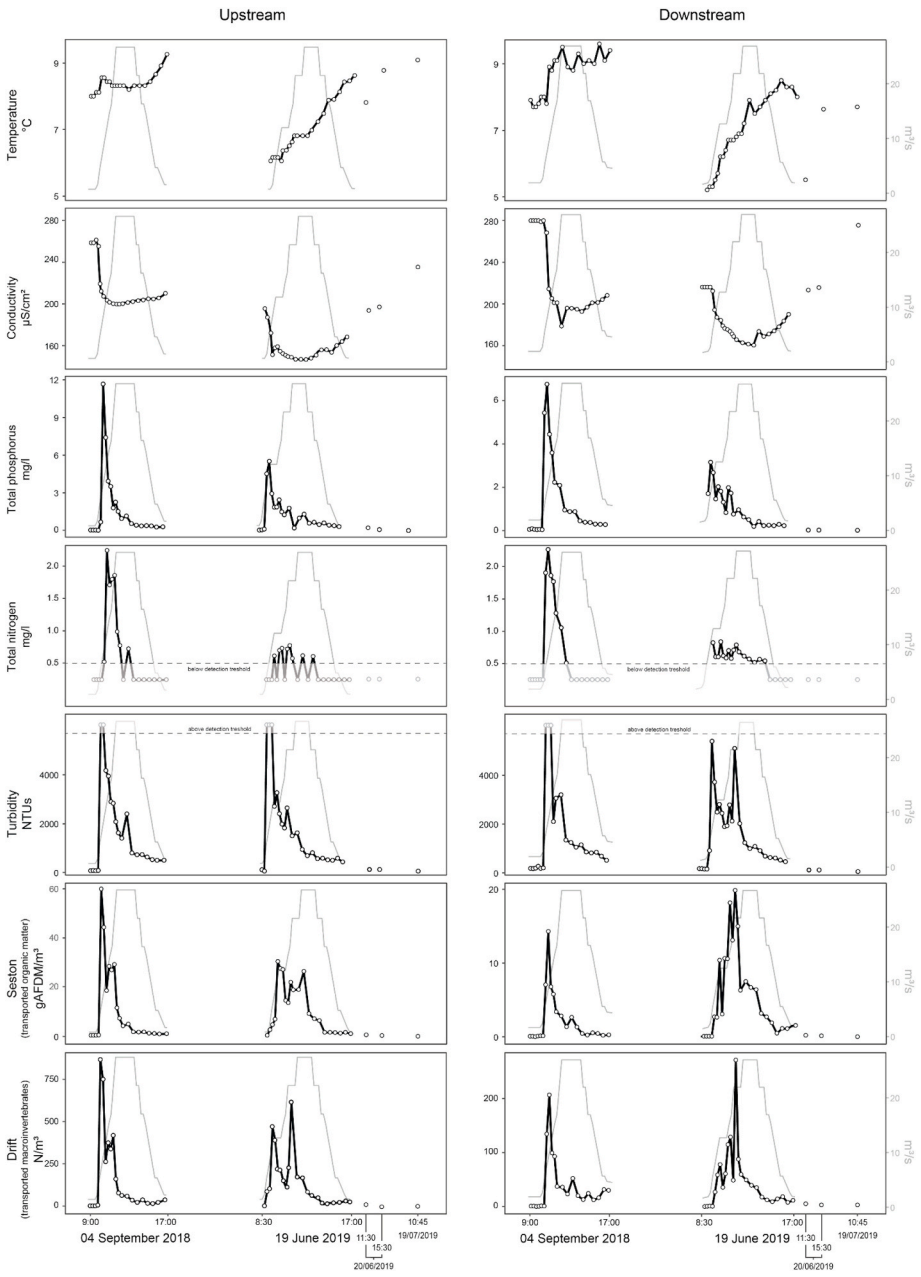

Fig. 3. Measurements taken during the two floods upstream (site D) and downstream (site A) of the tributary Ova da Cluozza. From top to bottom: temperature, conductivity, total phosphorus, total nitrogen, turbidity, seston and macroinvertebrate drift (note the y-axis differences between left and right panels for total phosphorus, seston and drift). In these cases, y-axes were kept different to emphasize response patterns. The grey lines in the background show discharge (right y-axis on each panel). X-axis represents the timeline of the events (not to scale).

as confirmed by the measurements taken the day after the flood. In this case, water temperature inside the reservoir did not seem to differ from water temperature in the stream.

Conductivity showed comparable patterns between reaches, but differences between years (Fig. 3). Water input from Ova da Cluozza added +10 µS/cm^2 to downstream waters. In 2018, water release from the dam caused a decrease from baseline values between 270 and 280 to 200–210 µS/cm^2. Downstream, we measured a drop in conductivity to a minimum value of 185 µS/cm^2 at maximum discharge, which corresponded to the second turbidity peak (see below) and an increase of ~0.5 °C in temperature. In 2019, baseline values of 200–210 µS/cm^2 decreased to 150–160 µS/cm^2 during the flood at both reaches, then returned to pre-flood values as soon as discharge started decreasing.

Total phosphorus (TP) sharply increased at both reaches during each flood at an early stage of the rising limb (Fig. 3). Maximum TP differed between reaches, decreasing by ~ half below the tributary (11.6–6.8 mg/l in 2018, 5.5 to 3.2 mg/l in 2019). This increase on the rising limb also was observed for total nitrogen (TN), which showed a sharp increase in 2018 at both reaches (with peaks around 2.2–2.3 mg/l), while values were always below 1.0 mg/l in 2019.

Turbidity quickly exceeded the instrument detection threshold (6000 NTUs) in 2018 at both reaches during the rising limb of the flood (Fig. 3). This increase was related to fine sediments being released from the dam along with fine sediments and organic matter being mobilized from the streambed in response to the increase in discharge. Response patterns between reaches were compatible with the flood wave moving downstream. Secondary turbidity peaks were observed at both reaches as well. In 2019, turbidity responded similarly to 2018 at the upper reach. In contrast, we observed two marked peaks below the tributary in 2019, the first with the increase in flow from the flood, the second as discharge increased to the maximum release value of 25 m^3/s.

3.1.2. *Drift and seston during the floods*

Transported organic matter (seston) and macroinvertebrates (drift) showed corresponding patterns during both floods, where benthic organic matter and macroinvertebrates were entrained in the flow as the

water level increased (Fig. 3). In 2018, early peaks in seston and drift occurred simultaneously with peaks in turbidity, TP, and TN; i.e., during the early stages of the flood at ~ 5–10 m^3/s discharge. Above the tributary, the first seston (~60 g/m^3) and drift (~800 ind/m^3) peak was followed shortly after by a second, less marked peak (~30 g/m^3 and ~400 ind/m^3, respectively) that corresponded to the maximum flood discharge. Below the tributary, seston and drift showed comparable response patterns (first peak of ~15 g/m^3 and ~200 ind/m^3; second peak of ~3 g/m^3 and ~50 ind/m^3, respectively). The slower rising limb in flood 2019 resulted in a more gradual response in seston and drift than in 2018. Above the tributary, a double peak in drift (~500 and ~600 ind/m^3, respectively) followed the first two discharge increments (~10–20 m^3/s) and dropped shortly after to <100 ind/m^3. Seston concentration reached ~30 g/m^3 during the first increment and remained at15-25 g/m^3, showing two additional peaks with the second and last increase in discharge.

The total organic matter transported during the floods was 3197 and 4938 kg above the tributary, and 699 and 3044 kg below the tributary, in 2018 and 2019, respectively (Fig. 3). Total macroinvertebrate drift above the tributary was around 45–48 × 10^6 individuals during both floods (Table 1). Below the tributary in 2019, we recorded almost double the number of drifting macroinvertebrates than in 2018 (~13 and ~23 × 10^6 in 2018 and 2019, respectively) (Table 1). Gammaridae represented the largest fraction in the drift, being around 50% or higher at all sites in both floods. The remaining drift was composed of Chironomidae, Leuctridae, Baetidae, and Ephemeroptera other than Baetidae (mostly Heptagenidae). Lastly, Gammaridae and Chironomidae drift patterns corresponded to those of seston, reflecting their inclination to passive drift (Fig. 4a and c). Baetidae, Nemouridae, and Heptgenidae/Rhyacophilidae, in contrast, showed both a passive response to increasing discharge and an active response as discharge receded (Fig. 4b and d). However, this response was not uniform and mediated by location, abundance, and shape of the flood hydrograph.

Background drift for the entire study section was calculated based on the first three driftsamples from 2018 from both reaches, first three driftsamples from 2019 (only downstream, as the first sample from upstream was collected as the flood already started – see Fig. 3), and from three drift samples collected four weeks after the flood at both reaches. Results show very low background drift densities (1.7 ± 0.5 N/m^3), mostly constituted by Chironomidae (1.33 ± 0.45 N/m^3), Simulidae (0.12 ± 0.04 N/m^3), and Baetidae (0.1 ± 0.03 N/m^3), with the sporadic presence of other taxa.

3.2. Before/after effects of the floods

3.2.1. Benthic samples and sediment respiration

ANOVA test on periphyton data revealed significant differences for date ($p < 0.001$) and the interaction date × reach ($p < 0.001$). Before the flood in 2018, periphyton biomass was on average higher above than below the tributary (16.8 vs 10.7 gAFDM/m^2, respectively) (Fig. 5a), albeit not significantly (Tukey's HSD $p = 0.09$). The 2018 flood significantly reduced periphyton biomass in upstream sites to ~ half (7.6 gAFDM/m^2, $p < 0.001$), and levels returned to pre-flood conditions within four weeks (16.7 gAFDM/m^2, AF-LAF $p < 0.01$; BF-LAF $p = 1$). Below the tributary, periphyton biomass remained at similar levels for the duration of the study, although slightly increasing after the flood (15.8 gAFDM/m^2) and returned to an intermediate level (13.7 gAFDM/m^2) within four weeks. In 2019, patterns were similar at both reaches with no significant differences among sampling dates (Fig. 5a). Before the 2019 flood, periphyton biomass was significantly different to that found before the 2018 flood (Tukey's HSD $p < 0.001$ upstream and $p < 0.01$ downstream), approximately 2/3 lower (5.1 gAFDM/m^2 upstream and 4.2 downstream). There was no effect of the flood on periphyton biomass in 2019 at both reaches, and biomass almost doubled four weeks after the flood to 9.8 and 7.3 gAFDM/m^2, respectively, upstream and downstream (Tukey's HSD test AF-LAF, $p < 0.001$ and $p < 0.01$, respectively), following higher growth rates during summer months. Periphyton biomass upstream LAF was also significantly different from BF (Tukey's HSD $p < 0.01$).

The ANOVA test for benthic CPOM showed no significant difference related to date, reach, or their interaction. CPOM response pattern varied greatly between sites and floods (Fig. 5b). Benthic FPOM patterns were similar to those of periphyton (Fig. 5c). ANOVA test revealed significant differences for date ($p < 0.001$) and the interaction date × reach ($p < 0.05$). Upstream, the 2018 flood reduced FPOM (Tukey's HSD BF-AF, $p < 0.001$), then it increased four weeks after the flood (Tukey's HSD AF-LAF, $p < 0.05$). Downstream in 2018, FPOM levels remained relatively stable between 1.2 and 1.6 gAFDM/m^2. In 2019, both reaches show an increase in FPOM over time, and the flood had no significant effect.

We found that macroinvertebrate density differences were significant for date ($p < 0.001$) and reach ($p < 0.01$) (Fig. 5d). Before the 2018 flood, Tukey's HSD test revealed differences between sites ($p < 0.05$), with higher densities upstream. The impact of the flood was most evident upstream, where density went from ~5000 to ~100 ind/m^2, but density (at ~7000 ind/m^2) recovered to or exceeded pre-flood levels within four weeks (Tukey's HSD BF-AF $p < 0.001$; AF-LAF, $p < 0.001$; BF-LAF, $p = 1.0$). Downstream showed a similar pattern, however, the impact of the flood was smaller (~1000–~250 ind/m^2) and not significant, and density reached ~4000 ind/m^2 within four weeks after the flood (Tukey's HSD AF-LAF, $p < 0.001$). Before the 2019 flood, baseline densities were extremely low at both sites and significantly different to those found in 2018 (~200 and ~50 ind/m^2, respectively, upstream and downstream; tukey's HSD in both cases $p < 0.01$), and remained comparably low after the flood (~400 and ~80 ind/m^2). Four weeks after the flood, densities were significantly higher (~8000 and ~2300 ind/m^2) (Tukey's HSD upstream AF-LAF and BF-LAF, both $p < 0.01$; downstream AF-LAF, $p < 0.01$ and BF-LAF, $p < 0.001$).

Table 1
Taxonomic composition of macroinvertebrates in the (cumulative) drift during each flood (total number of individuals x 10^6).

		2018				2019			
		Upstream		Downstream		Upstream		Downstream	
Order	Taxa	N (× 10^6)	%	N (× 10^6)	%	N (× 10^6)	%	N (× 10^6)	%
Amphipoda	Gammaridae	28.8	62.8	6.6	51.1	24.9	51.5	11.4	49.6
Diptera	Chironomidae	5.9	12.8	1.3	10.1	11.0	22.9	2.8	12.2
	Other Dipt.	0.6	1.4	0.5	4.2	0.2	0.3	0.1	0.6
Ephemeroptera	Baetidae	1.5	3.2	1.6	12.3	4.2	8.7	1.1	4.8
	Other Ephem.	6.4	14.0	1.5	12.0	1.0	2.0	1.3	5.6
Plecoptera	Nemouridae	0.2	0.4	0.1	0.5	4.4	9.1	2.3	9.8
	Leuctridae	0.9	1.9	0.8	6.0	1.7	3.5	2.5	10.7
	Other Plecopt.	0.6	1.2	0.1	0.8	0.0	0.0	0.2	0.8
	Other taxa	1.1	2.3	0.4	3.0	0.9	1.9	1.4	5.9
	Total	46.0	100	12.9	100	48.3	100	23.1	100

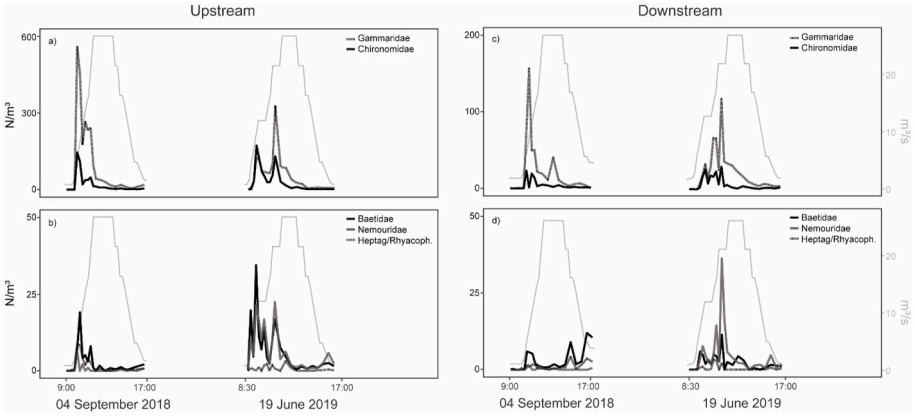

Fig. 4. Transported macroinvertebrate taxa (drift) during the two floods upstream (site D) and downstream (site A) of the tributary Ova da Cluozza (note the y-axis differences between top left and right panels). The grey lines in the background is the discharge during each flood (right y-axis on each panel).

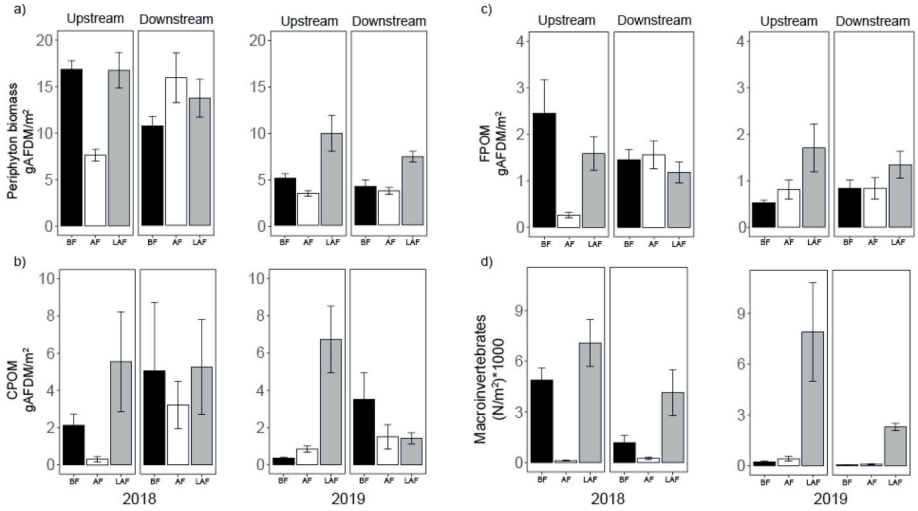

Fig. 5. Mean and standard error of benthic samples collected before (BF), after (AF) and four weeks after (LAF) the floods in 2018 and 2019, where a) periphyton biomass (gAFDM/m^2), b) CPOM biomass (gAFDM/m^2), c) FPOM biomass (gAFDM/m^2) and d) macroinvertebrate density (N/m^2).

Macroinvertebrate community composition (Table 2) varied greatly between reaches before the flood in 2018, with marked dominance of Gammaridae in the upstream reach, as opposed with the higher occurrence of Heptagenidae, Baetidae and Plecoptera downstream. The flood had an impact on taxa richness in upstream riffle habitats, while it remained substantially unchanged downstream. Four weeks after the flood, communities recovered to a similar pre-flood composition, with a notable increase of Leuctridae density in both reaches, and Simulidae downstream. In 2019, pre-flood community composition and density were strongly influenced by the snowmelt-induced disturbance in both reaches. Community composition was substantially left unchanged by the flood, with some density variations. After four weeks, community composition was dominated at both sites by Chironomidae and Simulidae. This determined notable differences in relative densities from those observed before the 2018 flood, at a similar time (end of August – beginning of September).

Sediment respiration responses to the floods differed significantly among dates ($p < 0.001$), reaches ($p < 0.001$), and their interaction ($p < 0.001$), (Fig. 6a). Before the flood in 2018, sediment respiration was, on average, four times higher upstream than downstream (Tukey's HSD $p < 0.001$). Sediment respiration upstream of the tributary was reduced by the flood, although not significantly (Tukey's HSD $p = 0.45$), while it remained the same downstream (Tukey's HSD $p = 0.99$). In 2019, sediment respiration in the upstream site was significantly lower than that found before 2018 flood (Tukey's HSD $p < 0.001$). The 2019 flood enhanced sediment respiration at both reaches, albeit significantly only upstream (Tukey's HSD $p < 0.05$). Concentration of LPOM differed significantly among dates ($p < 0.001$), while APOM differed significantly among reaches ($p < 0.01$) and dates ($p < 0.001$). In 2018, before the flood, the loose organic matter content (LPOM) of sediments upstream was double that of downstream sediment, although not significantly (Tukey's HSD $p = 0.16$); after the flood, levels were similar in both reaches (Fig. 6c). The flood significantly reduced LPOM content at both sites (respectively, Tukey's HSD $p < 0.001$ upstream and $p < 0.05$ downstream), while attached organic matter (APOM) decreased at both sites after the flood, although not significantly (Fig. 6b). In 2019, both reaches had similarly low LPOM concentrations (Fig. 6c), which differed significantly from those in 2018 before the flood only in the upstream reach (Tukey's HSD $p < 0.001$). LPOM concentrations remained similar after the 2019 flood (all Tukey's HSD $p \sim 0.95$). This flood significantly reduced only APOM in the upstream reach ($p < 0.01$). Concentrations of APOM before 2018 and 2019 floods were comparable at both sites. The content of APOM in sediments was generally comparable between reaches and before each flood (min = 4.18; max = 5.66), and was reduced ~ 1 g/kg after the floods (Fig. 6b). We found that respiration and LPOM concentrations were highly correlated before the floods ($r = 0.57$, $p < 0.001$) but not after ($r = 0.02$, $p = 0.89$), and that respiration was negatively correlated with APOM after the flood ($r = -0.52$, $p < 0.01$)

Table 2
Benthic macroinvertebrate composition expressed as mean density (N/m^2) ± standard error and relative abundance (%) before (BF), after (AF) and four weeks after (LAF) the floods in 2018 and 2019, upstream and downstream of the tributary.

	2018						2019					
	Upstream			Downstream			Upstream			Downstream		
Taxa	BF	AF	LAF	BF	AF	LAF	BF	AF	LAF	BF	AF	LAF
Gammaridae	2119.3 ± 822.4 (43.4%)	58.7 ± 19.2 (51.6%)	3127.7 ± 997.6 (46.2%)	110.0 ± 50.8 (9.3%)	44.0 ± 32.4 (17.1%)	168.7 ± 98.7 (4.1%)	0.5 ± 0.5 (5%)	2.0 ± 1.0 (10.7%)	330.0 ± 106.8 (4.2%)	0.3 ± 0.2 (16.7%)	0.5 ± 0.2 (13.0%)	7.3 ± 6.7 (0.3%)
Baetidae	843.3 ± 337.1 (17.3%)	7.3 ± 4.2 (6.4%)	330 ± 125.8 (4.9%)	326.3 ± 124.3 (27.5%)	47.7 ± 21.6 (18.6%)	425.3 ± 99.6 (10.2%)	0	0	550.0 ± 162.8 (7.0%)	0	0	124.7 ± 24.1 (5.5%)
Heptagenidae	117.3 ± 27.3 (2.4%)	14.7 ± 6.7 (12.9%)	117.3 ± 31.8 (1.7%)	223.7 ± 79.7 (18.8%)	40.3 ± 17.5 (15.7%)	150.3 ± 19.0 (3.6%)	2.3 ± 1.6 (23.3%)	6 ± 2.8 (32.1%)	77.0 ± 18.5 (1.0%)	0.3 ± 0.2 (16.7%)	1.2 ± 0.6 (30.4%)	99.0 ± 18.5 (4.3%)
Rhyacophilid.	36.7 ±11.2 (0.7%)	7.3 ± 4.2 (6.4%)	260.3 ± 51.7 (3.8%)	33.0 ± 18.5 (2.8%)	7.3 ± 4.2 (2.9%)	143 ± 37.7 (3.4%)	0.2 ± 0.1 (1.7%)	0.7 ± 0.6 (3.6%)	40.3 ± 14.1 (0.5%)	0	0	14.7 ± 8.5 (0.6%)
Other Trichopt.	216.3 ± 149.7 (4.4%)	0	29.3 ± 12.3 (0.4%)	0	3.7 ± 3.3 (1.4%)	0	0	0	14.7 ± 4.2 (0.2%)	0	0	3.7 ± 3.3 (0.2%)
Nemouridae	36.7 ± 11.2 (0.7%)	0	0	36.7 ± 21.8 (3.1%)	3.7 ± 3.3 (1.4%)	0	0	0	234.7 ± 76.7 (3.0%)	0	0	113.7 ± 29.5 (5.0%)
Leuctridae	451.0 ± 287.8 (9.2%)	3.7 ± 3.3 (3.2%)	1316.3 ± 416.6 (19.4%)	51.3 ± 35.4 (4.3)	14.7 ± 6.7 (5.7%)	1085.3 ± 312.3 (26.1%)	0	0	18.3 ± 8.1 (0.2%)	0	0	66.0 ± 16.4 (2.9%)
Other Plecopt.	462.0 ± 132.4 (9.5%)	0	315.3 ± 86.1 (4.7%)	238.3 ± 147.0 (20.1%)	7.3 ± 6.7 (2.8%)	498.7 ± 122.5 (12.0%)	0.8 ± 0.3 (8.3%)	6.8 ± 3.0 (36.6%)	66.0 ± 27.4 (0.8%)	0.3 ± 0.2 (16.7%)	1.0 ± 0.6 (26.1%)	3.7 ± 3.3 (0.2%)
Simulidae	47.7 ± 21.0 (1%)	0	234.7 ± 115.0 (3.5%)	91.7 ± 30.9 (7.7%)	11.0 ± 6.8 (4.3%)	1063.3 ± 715.0 (25.6%)	0	0	4825.3 ± 2452.1 (61.1%)	0	0	458.3 ± 118.2 (20.1)
Chironomidae	135.7 ± 43.82 (2.8%)	0	652.7 ± 433.5 (9.7%)	25.7 ± 13.1 (2.2%)	51.3 ± 16.9 (20%)	458.3 ± 83.2 (11.0%)	1.0 ± 0.5 (10%)	1.2 ± 0.4 (6.2%)	1514.3 ± 366.1 (19.2%)	0.5 ± 0.3 (25%)	0.2 ± 0.1 (4.3%)	1045.0 ± 101.3 (45.7%)
Other Diptera	253.0 ± 58.15 (5.2%)	14.7 ± 4.2 (12.9%)	62.3 ± 12.1 (0.9%)	40.3 ± 18.3 (3.4%)	7.3 ± 4.2 (2.8%)	139.3 ± 53.3 (3.3%)	2.3 ± 0.8 (23.3%)	1.3 ± 0.7 (7.1%)	47.7 ± 12.1 (0.6%)	0.2 ± 0.1 (8.3%)	0.7 ± 0.2 (17.4%)	66.0 ± 24.3 (2.9%)
Other taxa	165.0 ± 39.09 (3.4%)	7.3 ± 4.2 (6.4%)	319.0 ± 215.3 (4.7%)	11.0 ± 6.9 (0.9%)	18.3 ± 10.9 (7.1%)	18.3 ± 13.1 (0.4%)	2.8 ± 1.0 (28.3%)	0.7 ± 0.4 (3.6%)	176 ± 99.3 (2.2%)	0.3 ± 0.2 (16.7%)	0.3 ± 0.4 (8.7%)	282.3 ± 117.5 (12.4%)

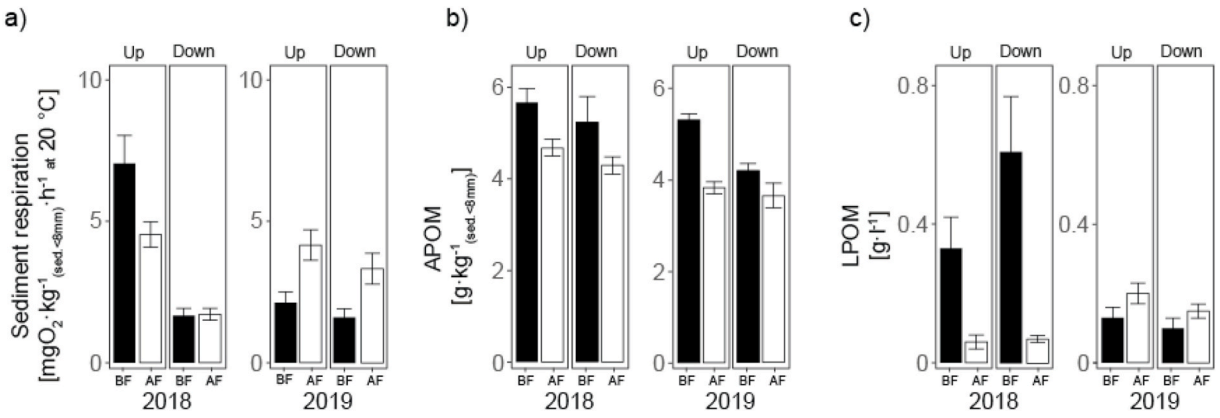

Fig. 6. a) Sediment metabolism (mean, standard error) expressed as the difference in dissolved $mgO_2.kg^{-1}_{(sed.<8mm)}.h^{-1}$ at 20 °C after at least 4 h incubation, b) APOM (attached POM) expressed as $g.kg^{-1}_{(sed.<8mm)}$, and c) LPOM (loose POM) expressed as $g.l^{-1}$ of sediments incubated in the respiratory tubes (n = 3 for each sampling site) for estimates of sediment metabolism before (BF) and after (AF) the floods in 2018 and 2019, upstream (Up) and downstream (Down) Ova da Cluozza confluence.

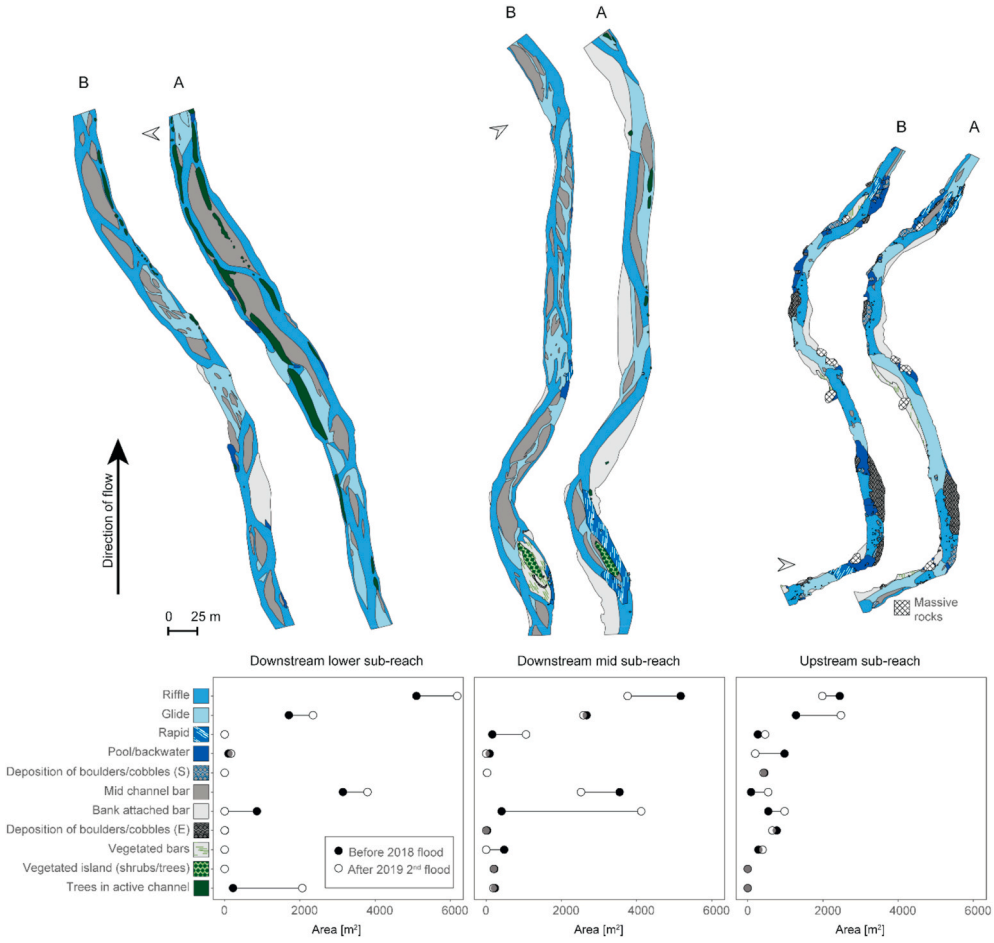

Fig. 7. Geomorphic units and sub-units assemblage (GUS basic level) of the three sub-reaches before 2018 flood (B) and after 2nd 2019 flood (A) (for sub-reach location along the study reach see Fig. S1 in supplementary material). The lower panel shows changes in geomorphic units and sub-units areas across the same period. (S) = partly submerged, (E) = emerged.

but not before (r = 0.13, p = 0.48). LPOM and APOM content were also significantly correlated before (r = 0.64, p < 0.001) but not after the floods (r = −0.01, p = 0.95).

3.2.2. *Flood induced changes in channel morphology*

The two reaches showed substantial baseline morphological and morphodynamics differences (Fig. S1 in supplementary material) in response to the experimental floods. Above the tributary, the reach is characterized by a narrow valley and showed signs of flow regulation and sediment deficit, with instream emergent sediment patches limited in extent and vegetated side bars disconnected from the active channel. Instream vegetation patches were limited in number and size (Table 3)

Table 3
Number (N) and mean area (± standard deviation) of macro-units (emergent (E) sediment, submerged channel and vegetation present in the active channel) before (2018) and after each flood in the two study reaches, resulting from the broad level GUS analysis (maps shown in Fig. S1 in supplementary material).

	2018 (25 m^3/s)				2019 (25 m^3/s)		2019 (40 m^3/s)	
	Before		After		After		After	
	Mean area ±sd (m^2)	*N (tot m^2)*	*Mean area ±sd (m^2)*	*N (tot m^2)*	*Mean area ±sd (m^2)*	*N (tot m^2)*	*Mean area ±sd (m^2)*	*N (tot m^2)*
Upstream sediment (E)	19 ± 52	140 (2635)	12 ± 42	245 (2957)	17 ± 59	165 (2751)	23 ± 65	135 (3171)
Upstream vegetation	64 ± 31	4 (255)	15 ± 19	8 (118)	10 ± 25	28 (288)	9 ± 12	8 (78)
Downstream sediment (E)	98 ± 152	143 (14065)	93 ± 384	186 (17418)	131 ± 416	117 (15329)	170 ± 492	106 (18082)
Downstream vegetation	184 ± 349	15 (2764)	73 ± 198	45 (3274)	61 ± 160	89 (5434)	74 ± 165	70 (5151)
	Area (m^2)		*Area (m^2)*		*Area (m^2)*		*Area (m^2)*	
Upstream channel	8937		8878		9365		9169	
Downstream channel	23083		23215		27618		25482	

Table 4
Mean width (±standard deviation), area, and submerged/emerged units ratio of the active channel, in the three sub-reaches (one upstream, two downstream) based on the analysis of changes in geomorphic units and sub-units (GUS basic level) after the three floods (maps and data shown in Fig. 7). For the location of the reaches refer to Fig. S1 in supplementary material.

	Upstream		Downstream mid		Downstream lower	
	Before flood 2018	After 2nd flood 2019	Before flood 2018	After 2nd flood 2019	Before flood 2018	After 2nd flood 2019
Sub-reach length *(m)*	486		546		491	
Width *(m)* mean ± sd	14 ± 4	15 ± 3	23 ± 5	26 ± 3	24 ± 2	29 ± 7
Area *(m^2)*	7128	7873	12656	13809	11788	14556
Submerged/emerged	0.31	0.46	0.57	0.43	0.52	0.80

and mostly comprised of small shrubs and grass. With the floods, upstream emerged sediment and vegetation patches were relatively stable in terms of mean size, with limited changes in number and area. The analysis of geomorphic units in the upstream sub-reach confirmed no major morphological changes (Fig. 7, Table 4), and limited lateral dynamics. Active channel width and surface remained substantially unchanged after the floods, showing only small increases related to local redistribution of sediments and exposure of bank attached sediment patches (Fig. 7). Before the floods, the sub-reach was characterized by the presence of relatively large areas of slow-flow (pools/backwater), some of which were formed by large wood deposits, that were greatly reduced after the floods. Riffle surface was also reduced, in favour of glides, as a consequence of gravel-sized sediment deposition in the channel. This sub-reach was characterized by the presence of partly submerged boulder-cobble depositions that remained substantially unchanged after the floods.

In the downstream reach, the valley gradually opens up and lateral controls give room to the alluvial valley. Here, sediment is supplied by Ova da Cluozza, which is also responsible for enhanced channel dynamics downstream. A braided channel formed across large patches of emergent sediment in the form of bars and islands. Instream vegetation here is mostly represented by trees and shrubs on vegetated islands and banks. A large and a mid-sized vegetated island characterized the area just below the confluence (Fig. S1 in supplementary material). With the floods, downstream emergent sediment patches gradually increased in size (Table 3), and the total surface occupied by emergent sediments had increased after all floods from 14,065 to 18,082 m^2 with some fluctuations between floods (Table 3). This increase in sediment bar size and surface was associated with a simplification of channel morphology, mainly in the mid sub-reach of the downstream reach (Fig. 7), where scattered minor bars gave room to larger, bank-attached bars, and the development of a mostly single-thread channel. In this sub-reach, mean active channel width and area slightly increased (Table 4), mostly related to lateral deposition. After the floods, riffle area declined in favour of rapids, while other submerged units area remained substantially unchanged. This riffle-rapid turnover was driven by erosive dynamics in the area surrounding one of the vegetated islands (Fig. 7), as indicated by the removal of the vegetated sediment surrounding the island.

The floods activated interesting lateral dynamics in the lower sub-reach as well, with the formation and stabilization of a lateral secondary channel on the left bank (Fig. 7), and the inundation of the right bank, with an associated increase of vegetation (trees) presence in the active channel. The formation of this secondary channel after the first 2019 flood, and consolidation after the second 2019 flood, increased the active channel mean width and area, with a sharp growth of submerged areas (glides and riffles) (Table 4 and Fig. 7). This was associated with the formation of two large mid-channel bars (Fig. 7).

4. Discussion

4.1. Immediate flood responses

4.1.1. Physico-chemistry

Transient physico-chemical changes of surface waters during an experimental flood are a function of reservoir characteristics. Patterns of temperature and conductivity change measured during the flood reflect temperature and conductivity of reservoir waters that vary depending on the season. Small reservoirs like Ova Spin are generally characterized by short hydraulic residence time that strongly limit functional processes in the reservoir. For some nutrients, however, even short residence times will result in some sequestration. For example, phosphorus (burial) and to a lesser extent nitrogen (denitrification and burial) will accumulate in reservoir sediments (Maavara et al., 2020; Maranger et al., 2018). During the study floods, deep-water releases suspended and mobilized reservoir sediments. TN and TP concentrations measured during the floods appeared to be tightly coupled with sediment flushing, as observed also in previous studies on the system (e.g., Kevic et al., 2018). Suspended sediment load measured as turbidity was higher in the initial ramping phase, as fine sediments were flushed with reservoir

waters, and scoured from the streambed. Turbidity rapidly declined in 2–4 h time, confirming the limited capacity of experimental floods from Ova Spin to entrain large volumes of fines (Scheurer and Molinari, 2003).

While turbidity patterns were comparable between the two floods, TP and TN patterns differed greatly between floods, indicating the influence of season and time since a previous flood on nutrients adsorbed to sediments deposited in the reservoir. Transport TP data might suggest the occurrence of deposition along the study segment; here, ~6 and ~3 mg/l, respectively, were deposited in ~2 km during each flood. This large input of phosphorus might influence recovery patterns to experimental floods by subsidizing biofilm assemblages (Odum et al., 1979). Nutrient inputs during experimental floods could have important implications in nuisance algae management (e.g., Lessard et al., 2013; Uehlinger et al., 2003), but require more detailed studies on mechanisms of accrual.

4.1.2. Seston and drift

Temporal patterns of seston during each flood were generally consistent with those observed in previous floods in the upper Spöl (Jakob et al., 2003; Robinson, 2012; Robinson et al., 2004a) and lower Spöl (Kevic et al., 2018), and followed a typical hysteresis curve (i.e., a decline of response intensity over time) (Scheffer et al., 2001). Although floods had identical peak flows and overall released comparable volumes of water (~5×10^5 m^3), we observed variability in flow-dependent entrainment and transportation of seston, where differences in the ramping rate and pre-flood conditions (this last factor also supported by benthic samples and field observations, see par 3.2) appear to be important in shaping the flood response (Fig. 3). The 2018 flood had a shorter duration and a much steeper rising limb than the 2019 flood. During the 2018 flood, seston response was earlier and stronger and peaked at a lower discharge compared to the 2019 flood, which had stepwise increases in discharge. During the flood of 2019, seston response also could have been influenced by pre-flood conditions determined by the intense spring snowmelt (Fig. 5b and c; see also section 4.2.2 below).

We hypothesize that the lateral contribution of snowmelt water from side valleys and small tributaries, as well as increased discharge from the tributary Ova da Cluozza, likely caused a moderate disturbance in the system (both study reaches), which influenced the distribution of organic matter and macroinvertebrates in the channel before the 2019 flood (discharge of Ova da Cluozza during the study period is reported in Fig. 2). Benthic samples collected before the 2019 flood had extremely low macroinvertebrate abundances in riffle habitats at both study sites (Fig. 5d, Table 2). A closer look revealed that a higher number of macroinvertebrates moved from these areas into lateral habitats (GC and CTR personal observation), which can be important refugia during disturbance events (e.g., Lancaster and Hildrew, 1993a). As drift density and taxa richness were comparable between floods, we suggest that macroinvertebrates were present at similar densities as found before the earlier flood (2018), (Table 1), but likely distributed mostly in refugia habitat. Secondary peaks of drifting macroinvertebrates, seston and turbidity, as observed in other large-magnitude experimental floods in the system (>12 m^3/s peaks) (see Kevic et al., 2018; Robinson, 2012; Robinson et al., 2004b), occurred at both sites during the first flood at approximately peak discharge. These secondary peaks resulted from lateral erosion of scree slopes, bank inundation, and secondary mobilization of the streambed, which likely recruited organisms from hyporheic and side-channel refugia (Lancaster and Hildrew, 1993b; Matthaei et al., 2000; Stubbington, 2012), as well as mobilizing organic matter from banks.

Drift was dominated by Gammaridae (*G. fossarum* being the only species present in the system). Flood-driven drift composition quickly diverged from background drift in the system - mostly constituted by Chironomidae, Simulidae and Baetidae at low densities, with the sporadic presence of Gammaridae and other taxa - and converged to resemble benthic composition (Gibbins et al., 2007) with the addition of other limnophilic taxa (e.g., Psychodidae). Taxa drift response varied across floods and locations (Fig. 4). Response to high flows has been shown to be strongly taxon- and habitat-specific, depending on a combination of habitat structure, substrate stability, and physical or behavioral attributes that confer resistance (Holomuzki and Biggs, 2003; Irvine and Henriques, 1984; Mcmullen and Lytle, 2012; Naman et al., 2017). In our study, Chironomidae and Gammaridae showed a purely passive response, with patterns closely resembling those of organic matter. Baetidae, Nemouridae, and Heptagenidae show mixed patterns of response, where the initial passive response in some cases was followed by a growing number of drifting individuals as flood waters receded. Poff et al. (2018) observed that some traits, such as high mobility (i.e., Baetidae) are important for the persistence of taxa after disturbance, and can be determinant in habitat recolonization and stranding avoidance during water recession. However, this response was variable across floods and sites, suggesting an influence of morphology and water recession velocity (Bond and Downes, 2003; Sedell et al., 1990). The latter response observed might indicate that active drift was initiated by receding water as a mechanism to recolonize instream habitats after disturbance. Changes in water temperature following deep-water releases (so-called thermopeaking; Zolezzi et al., 2011), as during 2018 flood, could add up to flow effects and influence taxon-specific drift responses (Schülting et al., 2016).

4.2. Tributary effect

4.2.1. Morphological dynamics and sediment respiration

Although sedimentological differences were not quantitatively assessed in this study (but see Mathers et al., 2021), the environmental discontinuity (*sensu* Rice et al., 2001) generated by the presence of the tributary appears evident. Above the tributary, morphology is dominated by a single thread channel with riffle-pool sequences, and stable flow conditions associated with a sediment deficit suggest channel degradation and a reduction of lateral dynamics. In this reach, the lack of a major sediment source resulted in negligible morphological changes in response to experimental floods. However, a closer look at instream changes (Fig. 7) suggests that the intense snowmelt before the 2019 flood activated lateral sediment sources also above the confluence with Ova da Cluozza. These sediments were redistributed during the 2019 floods and caused observable changes in habitat structure. A substantial increase in glides, and pools reduction, occurred as a consequence of local gravel depositions, resulting in more homogeneous habitat conditions. However, these changes did not alter the overall geomorphic unit composition of the reach. The floods did not result in enhanced lateral dynamics, suggesting that channel incision had inevitably disconnected the channel from riparian areas. These results highlight the influence of river regulation on morphology, as well as the importance of local sediment sources (i.e., scree slopes and minor tributaries) in sediment-deprived reaches (Petts, 1979) for instream physical habitat rejuvenation through disturbance.

Further downstream, the sediment input from Ova da Cluozza promotes braiding of the channel across gravel bars and the existence of a wider floodplain with vegetated islands. In unregulated alpine rivers, sediment input by the tributary would be regularly mobilized and redistributed by the receiving channel (Guillén Ludeña et al., 2017), often simultaneously, as high flow events would affect the entire catchment. At the Spöl – Ova da Cluozza confluence, sediments accumulate and are partly redistributed solely during experimental floods, as the residual flow on the Spöl does not have enough competence for sediment mobilization. The study floods stimulated morphological processes below the tributary, where patterns of erosion and deposition of sediments, and reorganization of morphological units, were evident. During the study, we witnessed lateral channel movements because of sediment redistribution, the formation of a secondary channel, and the inclusion of bank vegetation in the active channel.

Experimental floods, when coupled with sediment input, can maintain patch dynamics in stream ecosystems (Matthaei et al., 1999a; Townsend, 1989). Stahly et al. (2019) observed the importance of sediment supply in combination with experimental floods in restoring fluvial habitats, however empirical studies in this sense are few. A previous study on this segment of river (Kevic et al., 2018) report that no major morphological changes (measurements based on permanent transects) occurred after the evident channel forming changes that followed the first floods (2000–2003; Mürle et al., 2003). Channel adjustments below a dam are gradual and occur over long timescales (Petts and Gurnell, 2005). In this lower section, lateral mobility could have been enhanced by aggradation with subsequent slope change over the years (Petts, 1984). The formation of secondary lateral channels and wet areas, with trees involved in channel dynamics within the floodplain, has an extraordinary value in increasing microhabitat heterogeneity in the reach, both for fish and macroinvertebrates (Benke and Wallace, 2003; Dolloff and Warren, 2003).

Sediment respiration showed response patterns consistent with the other benthic components (see below). The 2018 flood significantly reduced sediment respiration above the tributary, while leaving it unchanged below, and the 2019 flood resulted in an enhancement of respiration at both sites. In general, a flood's scouring effect removes surface POM and small particles, thus enhancing the permeability of sediments and promoting POM penetration into deeper sediments (Naegeli et al., 1995). Floods, by modifying local hydraulic characteristics of streambeds, can influence POM presence in the sediment, thus affecting respiration (Naegeli et al., 1995). Studies carried out during early experimental floods on the upper Spöl found that floods greatly enhanced respiration rates, but had no effect on POM sediment content (Uehlinger et al., 2003). With the 2018 flood, we observed significant removal of POM at both sites, but no significant change in 2019. The positive correlation observed between sediment respiration rates and loose POM indicates that, before floods, heterotrophic activity is sustained by this pool of resources. This result suggests that a rapid response to floods was mediated by a combination of scouring of the small fraction of POM and time since the last flood disturbance. However, we also found a negative correlation between attached POM and respiration rate after the flood. Further studies will need to estimate changes in vertical gradients of surface/subsurface exchange after experimental floods to better understand mechanisms that affect responses of sediment metabolism.

4.2.2. *Benthic responses*

The contrasting benthic responses to the floods, with marked differences above/below the tributary in 2018 and 2019, confirm that short-term disturbance history is a strong determinant of resource distribution and macroinvertebrate community structure (Matthaei et al., 1999a). Below the confluence, periodic disturbances generated by Ova da Cluozza maintain the Spöl river in a dynamic state (i.e., shifting mosaic theory) and influence resistance and resilience of its ecological components. On the other hand, the constant residual flows released from the dam maintain stable environmental conditions above the confluence, with consequent ecological re-arrangements (Bunn and Arthington, 2002). These differences in hydrological conditions determine ecological baseline dissimilarities above and below the tributary, and determine different ecological response patterns to experimental floods, as observed before the 2018 flood. However, these dissimilarities were reduced after the 2019 intense snowmelt event that affected both reaches. The intense snowmelt induced extraordinary, although recurrent at small frequency, hydrological conditions in the system, as testified by the hydrological data from Ova da Cluozza (Fig. 2). The discharge peak generate by this event on Ova da Cluozza was the 4th highest since 2000, with an estimated 10 years return period (FOEN – Federal Office for the Environment flood statistics, available at www.hydrodaten.admin.ch). Based on field observations and the results from this study, we suggest that a major disturbance event was associated with snowmelt also above the confluence.

In 2018, we observed a strong location effect (i.e., tributary effect) driven by differences in disturbance history between the upper and lower reaches. Between the dam and the confluence, the prolonged stable flow conditions with no natural floods resulted in dramatic responses to the experimental flood. Streambed disturbance during the flood resulted in periphyton scouring and mobilization of organic matter (FPOM and CPOM) (Robinson et al., 2018). Macroinvertebrate density decreased 25-fold, suggesting limited system resistance to flood. Periphyton and macroinvertebrate responses were compatible with that observed in previous experimental floods on another residual flow reach on the Spöl (Robinson et al., 2018). Below the confluence, the change in morphology associated with water/sediment input from the tributary and periodic flow disturbances resulted in less marked response patterns to the experimental flood. Sample variability appeared to be higher, reflecting patchiness in a more dynamic system (Matthaei et al., 1999b), and overall changes were limited and generally non-significant for most environmental variables. For instance, periphyton and benthic organic matter were not flushed from the reach, and macroinvertebrates, which had relatively low densities, were in proportion less affected by the flood than in the upper reach. Periphyton persistence in the downstream reach, as opposed to the drastic reduction in biomass in the upstream reach, could also depend on differences in the algal assemblage. As observed by Biggs and Thomsen (1995), algal species show different resistance to scouring events, thus suggesting potential adaptation differences to disturbance in algal communities.

In 2019, ecological response patterns were largely dissimilar to those of 2018. Baseline conditions at both reaches were influenced by the recent natural disturbance, thus the experimental flood had limited effect. In general, benthic components were comparable above/below the tributary before the flood, and responded with similar patterns to the flood, except for CPOM, which is usually patchy in its distribution (Small et al., 2008). Periphyton development, as well as formation and deposition of FPOM, followed a gradual increase over time at both sites, favored by stable flows after the flood events (Biggs, 1988; Webster et al., 1987).

The environmental discontinuity generated at the confluence generally marks shifts in macroinvertebrate assemblages (Katano et al., 2009; Rice et al., 2001), following changes in hydrological conditions and physical habitat structure and distribution. In our system, these baseline differences were evident in 2018. Stable flow conditions before the flood favored Gammaridae, which dominated benthic assemblages (~50%) above the tributary. Gammaridae colonized the Spöl after dam construction and are local indicators of habitat degradation associated with flow regulation (Robinson et al., 2003). Below the tributary, limited availability of suitable habitat and disturbance contributes to maintaining low Gammaridae density. In contrast, suitable habitats for EPT taxa (Ephemeroptera, Plecoptera and Trichoptera) are present and they comprise ~80% of the benthic assemblage, confirming the mitigation function of post-impoundment tributaries (Milner et al., 2019; Ward and Stanford, 1983).

In 2019, the pre-flood disturbance from snowmelt could have triggered migration of invertebrates towards refugia, e.g. hyporheos or side areas of the channel in both reaches, in effect acting as "natural" flood precursor, attenuating the difference between natural, "predictable" high flows and unanticipated experimental floods. The differential persistence of taxa after the flood suggests that river morphology and habitat structure likely influence community attributes of resistance to floods (Gjerløv et al., 2003; Holomuzki and Biggs, 2003; Townsend, 1989). Disturbance history, as observed by Effenberger et al. (2006), has a fundamental importance in determining the distribution of invertebrates in different stream habitats. However, Mcmullen and Lytle (2012) observed a systematic underestimation in density following disturbance events, thus further studies are needed to quantify the influence of morphology on resistance (and resilience) of stream macroinvertebrate communities across habitats.

After each flood, regardless of location, Simuliidae and Chironomidae recolonized the system at high densities (measured four weeks after), taking advantage of newly available habitats. A strong response of these two taxa was observed after the 2019 flood with cumulative density between 65 and 80%. Early instars of Leuctridae were also found in large quantities below the tributary four weeks after 2018 flood, marking the transition to a winter community. Above the tributary in 2018, Gammaridae returned to pre-flood densities in four weeks (~~3000 ind/m^2). Interestingly, Gammaridae densities in 2019 were low during the entire study period. High flood mortality, as well as sediment deposition that determined a riffle/glide transition habitat, can explain the persisting low Gammaridae densities.

5. Conclusions

In summary, flow alterations and sediment limitation strongly influenced ecological properties and ecosystem resilience/resistance in this regulated alpine river. We observed that the unregulated tributary Ova da Cluozza modified downstream river habitats and contributed to maintaining the system in a dynamic state by periodic, low-magnitude disturbance (Fig. 2). We observed that immediate responses to experimental floods on the Spöl were influenced by a combination of flood hydrograph, morphology, and disturbance legacy. Differential availability and accessibility of refugia likely played an important role in determining community resistance to floods, and recolonization patterns. Notably, we observed how an extraordinary disturbance event, associated with sediment input, influenced recovery patterns after experimental floods in a sediment-deprived residual flow reach. However, further studies are needed to investigate mechanisms of interactions between experimental floods, hydrology, and river morphology in influencing biotic responses, thereby increasing our understanding of the ecological effects of these large-scale flow experiments (Konrad et al., 2011). The differences in macroinvertebrate community resilience between years confirm the importance of flow disturbance in alpine systems to maintain habitat properties and limit non-native species.

Funding

This work was supported by the European Union's Horizon 2020 - Research and Innovation Framework Programme under the Marie Skłodowska-Curie grant agreement (MSCA) No. 765553 awarded to CTR, RMH, and GC.

Authors contribution

GC: Conceptualization; Methodology; Data curation; Formal analysis, Visualization; Writing - original draft; RMH: Funding acquisition; Resources; Supervision. MD: Methodology; Resources. SH: Methodology; Resources. CTR: Conceptualization; Funding acquisition; Methodology; Project administration; Writing - review & editing; Supervision.

Declaration of competing interest

The authors declare that they have no known competing financial interests or personal relationships that could have appeared to influence the work reported in this paper.

Acknowledgments

We thank the numerous students who took part in the sampling campaign during a EuroFLOW workshop in 2018. We thank Johannes Ortlepp (Hydra GmbH) for the planning of the floods, Christa Jolidon for field and laboratory work, and AUA lab for water chemistry analyses. We thank Samuel Wiesmann, Christian Rossi, Andreas Bruder and Virginia Ruiz-Villanueva for data and field support. We thank SNP and EKW for organizing and implementing the floods. We thank Gian Franco Kirchner (EKW) and FOEN for the hydrological data. We thank three anonymous reviewers and Guido Zolezzi for their thoughtful and constructive comments that improved this paper.

Appendix A. Supplementary data

Supplementary data to this article can be found online at https://doi.org/10.1016/j.jenvman.2021.114122.

References

Aristi, I., Arroita, M., Larrañaga, A., Ponsatí, L., Sabater, S., von Schiller, D., Acuña, V., 2014. Flow regulation by dams affects ecosystem metabolism in Mediterranean rivers. Freshw. Biol. 59 (9), 1816–1829.

Belletti, B., Rinaldi, M., Bussettini, M., Comiti, F., Gurnell, A.M., Mao, L., Nardi, L., Vezza, P., 2017. Characterising physical habitats and fluvial hydromorphology: a new system for the survey and classification of river geomorphic units. Geomorphology 283, 143–157. https://doi.org/10.1016/j.geomorph.2017.01.032.

Benke, A.C., Wallace, J.B., 2003. Influence of wood on invertebrate communities in streams and rivers. Am. Fish. Soc. Symp. 149–177, 2003.

Biggs, B.J.F., 1988. Algal proliferations in New Zealand's shallow stony foothills-fed rivers: toward a predictive model. SIL Proceedings 1405–1411. https://doi.org/10.1080/03680770.1987.11898031, 1922-2010 23.

Biggs, B.J.F., Thomsen, H.A., 1995. Disturbance of stream periphyton by perturbations in shear stress: time to structural failure and differences in community resistance. J. Phycol. 31, 233–241. https://doi.org/10.1111/j.0022-3646.1995.00233.x.

Bond, N.R., Downes, B.J., 2003. The independent and interactive effects of fine sediment and flow on benthic invertebrate communities characteristic of small upland streams. Freshw. Biol. 48, 455–465. https://doi.org/10.1046/j.1365-2427.2003.01016.x.

Bunn, S.E., Arthington, A.H., 2002. Basic principles and ecological consequences of altered flow regimes for aquatic biodiversity. Environ. Manag. 30, 492–507. https://doi.org/10.1007/s00267-002-2737-0.

Chapman, D.W., 1988. Critical review of variables used to define effects of fines in redds of large salmonids. Trans. Am. Fish. Soc. 117, 1–21. https://doi.org/10.1577/1548-8659(1988)117<0001:crovut>2.3.co.

Consoli, G., Haller, RM., Döring, D., Hashemi, S., Robinson, CT., 2021. Data for: Tributary effects on the ecological responses of a regulated river to experimental floods. Zenodo. https://doi.org/10.5281/zenodo.5555945.

Cross, W.F., Baxter, C.V., Donner, K.C., Rosi-Marshall, E.J., Kennedy, T.A., Hall, R.O., Wellard Kelly, H.A., Rogers, R.S., 2011. Ecosystem ecology meets adaptive management: food web response to a controlled flood on the Colorado River, Glen Canyon. Ecol. Appl. 21, 2016–2033. https://doi.org/10.1890/10-1719.1.

Davies, P.M., Naiman, R.J., Warfe, D.M., Pettit, N.E., Arthington, A.H., Bunn, Stuart E., 2012. Flow – ecology relationships : closing the loop on effective environmental flows. Mar. Freshw. Res. 133–141. https://doi.org/10.1071/MF13110.

Dolloff, C.A., Warren, M.L., 2003. Fish relationships with large wood in small streams. Am. Fish. Soc. Symp. 179–193, 2003.

Dudgeon, D., Arthington, A.H., Gessner, M.O., Kawabata, Z.-I., Knowler, D.J., Lévêque, C., Naiman, R.J., Prieur-Richard, A.-H., Soto, D., Stiassny, M.L.J., Sullivan, C.A., 2006. Freshwater biodiversity: importance, threats, status and conservation challenges. Biol. Rev. 81, 163. https://doi.org/10.1017/S1464793105006950.

Effenberger, M., Sailer, G., Townsend, C.R., Matthaei, C.D., 2006. Local disturbance history and habitat parameters influence the microdistribution of stream invertebrates. Freshw. Biol. 51, 312–332. https://doi.org/10.1111/j.1365-2427.2005.01502.x.

Gibbins, C., Vericat, D., Batalla, R.J., 2007. When is stream invertebrate drift catastrophic? The role of hydraulics and sediment transport in initiating drift during flood events. Freshw. Biol. 52, 2369–2384. https://doi.org/10.1111/j.1365-2427.2007.01858.x.

Gillespie, B.R., Desmet, S., Kay, P., Tillotson, M.R., Brown, L.E., 2015. A critical analysis of regulated river ecosystem responses to managed environmental flows from reservoirs. Freshw. Biol. 60, 410–425. https://doi.org/10.1111/fwb.12506.

Gjerløv, C., Hildrew, A.G., Jones, J.I., 2003. Mobility of stream invertebrates in relation to disturbance and refugia : a test of habitat templet theory. North Am. Benthol. Soc. 22, 207–223. https://doi.org/10.2307/1467993.

Golladay, S.W., Webster, J.R., Benfield, E.F., 1987. Changes in stream morphology and storm transport of seston following watershed disturbance. J. North Am. Benthol. Soc. 6, 1–11. https://doi.org/10.2307/1467519.

Grabowski, R.C., Gurnell, A.M., 2016. Hydrogeomorphology-ecology interactions in river systems. River Res. Appl. 32, 139–141. https://doi.org/10.1002/rra.2974.

Guillén Ludeña, S., Cheng, Z., Constantinescu, G., Franca, M.J., 2017. Hydrodynamics of mountain-river confluences and its relationship to sediment transport. J. Geophys. Res. Earth Surf. 122, 901–924. https://doi.org/10.1002/2016JF004122.

Harrison, L.R., Pike, A., Boughton, D.A., 2017. Coupled geomorphic and habitat response to a flood pulse revealed by remote sensing. Ecohydrology 10, 1–13. https://doi.org/10.1002/eco.1845.

Holomuzki, J.R., Biggs, B.J.F., 2003. Sediment texture mediates high-flow effects on lotic macroinvertebrates. J. North Am. Benthol. Soc. 22, 542–553. https://doi.org/10.2307/1468351.

Irvine, J.R., Henriques, P.R., 1984. A preliminary investigation on effects of fluctuating flows on invertebrates of the hawea river, a large regulated river in New Zealand. N. Z. J. Mar. Freshw. Res. 18, 283–290. https://doi.org/10.1080/00288330.1984.9516050.
Jakob, C., Robinson, C.T., Uehlinger, U., 2003. Longitudinal effects of experimental floods on stream benthos downstream from a large dam. Aquat. Sci. 65, 223–231. https://doi.org/10.1007/s00027-003-0662-9.
Jiménez-Segura, L.F., Palacio, J., Leite, R., 2010. River flooding and reproduction of migratory fish species in the Magdalena River basin, Colombia. Ecol. Freshw. Fish 19, 178–186. https://doi.org/10.1111/j.1600-0633.2009.00402.x.
Junk, W.J., Bayley, P.B., Sparks, R.E., 1989. The flood pulse concept in river-floodplain systems. Can. Spec. Publ. Fish. Aquat. Sci. 106, 110–127.
Katano, I., Negishi, J.N., Minagawa, T., Doi, H., Kawaguchi, Y., Kayaba, Y., 2009. Longitudinal macroinvertebrate organization over contrasting discontinuities: effects of a dam and a tributary. J. North Am. Benthol. Soc. 28, 331–351. https://doi.org/10.1899/08-010.1.
Kevic, M., Ortlepp, J., Mürle, U., Robinson, C.T., 2018. Effects of experimental floods in two rivers with contrasting valley morphologies. Fundam. Appl. Limnol./Arch. Hydrobiol. 2, 145–160. https://doi.org/10.1127/fal/2018/1177.
Kiernan, J.D., Moyle, P.B., Crain, P.K., 2012. Restoring native fish assemblages to a regulated California stream using the natural flow regime concept. Ecol. Appl. 22, 1472–1482. https://doi.org/10.1890/11-0480.1.
Konrad, C.P., Olden, J.D., Lytle, D.A., Melis, T.S., Schmidt, J.C., Bray, E.N., Freeman, M. C., Gido, K.B., Hemphill, N.P., Kennard, M.J., McMullen, L.E., Mims, M.C., Pyron, M., Robinson, C.T., Williams, J.G., 2011. Large-scale flow experiments for managing river systems. Bioscience 61, 948–959. https://doi.org/10.1525/bio.2011.61.12.5.
Lake, P.S., 2000. Disturbance, patchiness, and diversity in streams. J. North Am. Benthol. Soc. 19, 573–592. https://doi.org/10.2307/1468118.
Lancaster, J., Hildrew, A.G., 1993a. Characterizing in-stream flow refugia. Can. J. Fish. Aquat. Sci. 50, 1663–1675. https://doi.org/10.1139/f93-187.
Lancaster, J., Hildrew, A.G., 1993b. Flow refugia and the microdistribution of lotic macroinvertebrates. J. North Am. Benthol. Soc. 12, 385–393. https://doi.org/10.2307/1467619.
Lessard, J., Murray Hicks, D., Snelder, T.H., Arscott, D.B., Larned, S.T., Booker, D., Suren, A.M., 2013. Dam design can impede adaptive management of environmental flows: a case study from the Opuha Dam, New Zealand. Environ. Manag. 51, 459–473. https://doi.org/10.1007/s00267-012-9971-x.
Lytle, D.A., Poff, N.L., 2004. Adaptation to natural flow regimes. Trends Ecol. Evol. 19, 94–100. https://doi.org/10.1016/J.TREE.2003.10.002.
Maavara, T., Chen, Q., Van Meter, K., Brown, L.E., Zhang, J., Ni, J., Zarfl, C., 2020. River dam impacts on biogeochemical cycling. Nat. Rev. Earth Environ. 1, 103–116. https://doi.org/10.1038/s43017-019-0019-0.
Malmqvist, B., Rundle, S., 2002. Threats to the running water ecosystems of the world. Environ. Conserv. 29, 134–153. https://doi.org/10.1017/S0376892902000097.
Maranger, R., Jones, S.E., Cotner, J.B., 2018. Stoichiometry of carbon, nitrogen, and phosphorus through the freshwater pipe. Limnol. Oceanogr. Lett. 3, 89–101. https://doi.org/10.1002/lol2.10080.
Mathers, K.L., Robinson, C.T., Weber, C., 2021. Artificial flood reduces fine sediment clogging enhancing hyporheic zone physicochemistry and accessibility for macroinvertebrates. Ecol. Solut. Evid. 2 (4), e12103.
Matthaei, C.D., Arbuckle, C.J., Townsend, C.R., 2000. Stable surface stones as refugia for invertebrates during disturbance in a New Zealand stream. J. North Am. Benthol. Soc. 19, 82–93. https://doi.org/10.2307/1468283.
Matthaei, C.D., Peacock, K.A., Townsend, C.R., 1999a. Scour and fill patterns in a New Zealand stream and potential implications for invertebrate refugia. Freshw. Biol. 42, 41–57. https://doi.org/10.1046/j.1365-2427.1999.00456.x.
Matthaei, C.D., Peacock, K.A., Townsend, C.R., 1999b. Patchy surface stone movement during disturbance in a New Zealand stream and its potential significance for the fauna. Limnol. Oceanogr. 44, 1091–1102. https://doi.org/10.4319/lo.1999.44.4.1091.
Mcmullen, L.E., Lytle, D.A., 2012. Quantifying invertebrate resistance to floods: a global-scale meta-analysis. Ecol. Appl. 22, 2164–2175. https://doi.org/10.1890/11-1650.1.
Melis, T.S.E., 2011. Effects of three high-flow experiments on the Colorado river ecosystem downstream from glen canyon dam, Arizona. U.S. Geol. Surv. Circ. 1366, 147.
Milner, V.S., Yarnell, S.M., Peek, R.A., 2019. The ecological importance of unregulated tributaries to macroinvertebrate diversity and community composition in a regulated river. Hydrobiologia 829, 291–305. https://doi.org/10.1007/s10750-018-3840-4.
Mürle, U., Ortlepp, J., Zahner, M., 2003. Effects of experimental flooding on riverine morphology, structure and riparian vegetation: the River Spöl, Swiss National Park. Aquat. Sci. 65, 191–198. https://doi.org/10.1007/s00027-003-0665-6.
Naegeli, M.W., Hartmann, U., Meyer, E.I., Uehlinger, U., 1995. POM-dynamics and community respiration in the sediments of a floodprone prealpine river (Necker, Switzerland). Arch. Hydrobiol. 3, 339–347.
Naman, S.M., Rosenfeld, J.S., Richardson, J.S., Way, J.L., 2017. Species traits and channel architecture mediate flow disturbance impacts on invertebrate drift. Freshw. Biol. 62, 340–355. https://doi.org/10.1111/fwb.12871.
Nyberg, B., Buckley, S.J., Howell, J.A., Nanson, R.A., 2015. Geometric attribute and shape characterization of modern depositional elements: a quantitative GIS method for empirical analysis. Comput. Geosci. 82, 191–204. https://doi.org/10.1016/J.CAGEO.2015.06.003.
O'Connor, J.E., Duda, J.J., Grant, G.E., 2015. 1000 dams down and counting: dam removals are reconnecting rivers in the United States. Science 84 348, 496–497. https://doi.org/10.1126/science.aaa9204.
Odum, E.P., Finn, J.T., Franz, E.H., 1979. Perturbation theory and the subsidy-stress gradient. Bioscience 29, 349–352. https://doi.org/10.2307/1307690.
Olden, J.D., Konrad, C.P., Melis, T.S., Kennard, M.J., Freeman, M.C., Mims, M.C., Bray, E. N., Gido, K.B., Hemphill, N.P., Lytle, D.A., Mcmullen, L.E., Pyron, M., Robinson, C. T., Schmidt, J.C., Williams, J.G., 2014. Are large-scale flow experiments informing the science and management of freshwater ecosystems? Front. Ecol. Environ. 12, 176–185. https://doi.org/10.1890/130076.
Petts, G.E., 1984. Impounded Rivers: Perspectives for Ecological Management. John Wiley & Sons, Chichester, UK.
Petts, G.E., 1979. Complex response of river channel morphology subsequent to reservoir construction. Prog. Phys. Geogr. 3, 329–362. https://doi.org/10.1177/030913337900300302.
Petts, G.E., Gurnell, A.M., 2005. Dams and geomorphology: Research progress and future directions. Geomorphology 71, 27–47. https://doi.org/10.1016/j.geomorph.2004.02.015.
Poff, N.L., 2018. Beyond the natural flow regime? Broadening the hydro-ecological foundation to meet environmental flows challenges in a non-stationary world. Freshw. Biol. 63, 1011–1021. https://doi.org/10.1111/fwb.13038.
Poff, N.L., Allan, J.D., Bain, M.B., Karr, J.R., Prestegaard, K.L., Richter, B.D., Sparks, R.E., Stromberg, J.C., 1997. The Natural Flow Regime: a paradigm for river conservation and restoration. Bioscience 47, 769–784. https://doi.org/10.2307/1313099.
Poff, N.L.R., Larson, E.I., Salerno, P.E., Morton, S.G., Kondratieff, B.C., Flecker, A.S., Zamudio, K.R., Funk, W.C., 2018. Extreme streams: species persistence and genomic change in montane insect populations across a flooding gradient. Ecol. Lett. 21, 525–535. https://doi.org/10.1111/ele.12918.
Poiani, A., 2006. Effects of floods on distribution and reproduction of aquatic birds. Adv. Ecol. Res. 39, 63–83. https://doi.org/10.1016/S0065-2504(06)39004-6.
R Core Team, 2019. R: A Language and Environment for Statistical Computing.
Reid, A.J., Carlson, A.K., Creed, I.F., Eliason, E.J., Gell, P.A., Johnson, P.T.J., Kidd, K.A., MacCormack, T.J., Olden, J.D., Ormerod, S.J., Smol, J.P., Taylor, W.W., Tockner, K., Vermaire, J.C., Dudgeon, D., Cooke, S.J., 2019. Emerging threats and persistent conservation challenges for freshwater biodiversity. Biol. Rev. 94, 849–873. https://doi.org/10.1111/brv.12480.
Rice, S.P., Ferguson, R.I., Hoey, T.B., 2006. Tributary control of physical heterogeneity and biological diversity at river confluences. Can. J. Fish. Aquat. Sci. 63, 2553–2566. https://doi.org/10.1139/f06-145.
Rice, S.P., Greenwood, M.T., Joyce, C.B., 2001. Tributaries, sediment sources, and the longitudinal organisation of macroinvertebrate fauna along river systems. Can. J. Fish. Aquat. Sci. 58, 824–840. https://doi.org/10.1139/f01-022.
Robinson, C.T., 2012. Long-term changes in community assembly, resistance, and resilience following experimental floods. Ecol. Appl. 22, 1949–1961. https://doi.org/10.1890/11-1042.1.
Robinson, C.T., Aebischer, S., Uehlinger, U., 2004a. Immediate and habitat-specific responses of macroinvertebrates to sequential experimental floods. J. North Am. Benthol. Soc. 23, 853–867.
Robinson, C.T., Siebers, A.R., Ortlepp, J., 2018. Long-term ecological responses of the River Spöl to experimental floods. Freshw. Sci. 37 https://doi.org/10.1086/699481, 000–000.
Robinson, C.T., Tockner, K., Ward, J.V., 2002. The fauna of dynamic riverine landscapes. Freshw. Biol. 47, 661–677. https://doi.org/10.1046/j.1365-2427.2002.00921.x.
Robinson, C.T., Uehlinger, U., 2008. Experimental floods cause ecosystem regime shift in a regulated river. Ecol. Appl. 18, 511–526. https://doi.org/10.1890/07-0886.1.
Robinson, C.T., Uehlinger, U., Monaghan, M.T., 2004b. Stream ecosystem response to multiple experimental floods from a reservoir. River Res. Appl. 20, 359–377. https://doi.org/10.1002/rra.743.
Robinson, C.T., Uehlinger, U., Monaghan, M.T., 2003. Effects of a multi-year experimental flood regime on macroinvertebrates downstream of a reservoir. Aquat. Sci. 65, 210–222. https://doi.org/10.1007/s00027-003-0663-8.
Scheffer, M., Carpenter, S., Foley, J.A., Folke, C., Walker, B., 2001. Catastrophic shifts in ecosystems. Nature 413, 591–596. https://doi.org/10.1038/35098000.
Scheurer, T., Molinari, P., 2003. Experimental floods in the river Spöl, Swiss national Park: Framework, objectives and design. Aquat. Sci. 65, 183–190. https://doi.org/10.1007/s00027-003-0667-4.
Schülting, L., Feld, C.K., Graf, W., 2016. Effects of hydro- and thermopeaking on benthic macroinvertebrate drift. Sci. Total Environ. 573, 1472–1480. https://doi.org/10.1016/J.SCITOTENV.2016.08.022.
Sedell, J.R., Reeves, G.H., Hauer, F.R., Stanford, J.A., Hawkins, C.P., 1990. Role of refugia in recovery from disturbances: modern fragmented and disconnected river systems. Environ. Manag. 14, 711–724. https://doi.org/10.1007/BF02394720.
Small, M.J., Doyle, M.W., Fuller, R.L., Manners, R.B., 2008. Hydrologic versus geomorphic limitation on CPOM storage in stream ecosystems. Freshw. Biol. 53, 1618–1631. https://doi.org/10.1111/j.1365-2427.2008.01999.x.
Stähly, S., Franca, M.J., Robinson, C.T., Schleiss, A.J., 2019. Sediment replenishment combined with an artificial flood improves river habitats downstream of a dam. Sci. Rep. 9, 1–8. https://doi.org/10.1038/s41598-019-41575-6.
Stanford, J.A., Lorang, M.S., Hauer, F.R., 2005. The shifting habitat mosaic of river ecosystems. Internationale Vereinigung für theoretische und angewandte Limnologie: Verhandlungen 29 (1), 123–136.
Stubbington, R., 2012. The hyporheic zone as an invertebrate refuge: a review of variability in space, time, taxa and behaviour. Mar. Freshw. Res. 63, 293–311. https://doi.org/10.1071/MF11196.
Thompson, R.M., King, A.J., Kingsford, R.M., Mac Nally, R., Poff, N.L., 2018. Legacies, lags and long-term trends: effective flow restoration in a changed and changing world. Freshw. Biol. 63, 986–995. https://doi.org/10.1111/fwb.13029.
Townsend, C.R., 1989. The patch dynamics concept of stream community ecology. Source J. North Am. Benthol. Soc. 8, 36–50. https://doi.org/10.2307/1467400.

Turgeon, K., Turpin, C., Gregory-Eaves, I., 2019. Dams have varying impacts on fish communities across latitudes: a quantitative synthesis. Ecol. Lett. 22, 1501–1516. https://doi.org/10.1111/ele.13283.

Uehlinger, U., Kawecka, B., Robinson, C.T., 2003. Effects of experimental floods on periphyton and stream metabolism below a high dam in the Swiss Alps (River Spöl). Aquat. Sci. 65, 199–209. https://doi.org/10.1007/s00027-003-0664-7.

Uehlinger, U., Naegeli, M., Fisher, S.G., 2002. A heterotrophic desert stream? The role of sediment stability. West. North Am. Nat. 62, 466–473.

Vannote, R.L., Minshall, G.W., Cummins, K.W., Sedell, J.R., Cushing, C.E., 1980. the River continuum concept. Can. J. Fish. Aquat. Sci. 37, 130–137. https://doi.org/10.1139/f80-017.

Vinson, M.R., 2001. Long-term dynamics of an invertebrate assemblage downstream from a large dam. Ecol. Soc. Am. 11, 711–730. https://doi.org/10.1890/1051-0761(2001)011[0711:LTDOAI]2.0.CO;2.

Vörösmarty, C.J., McIntyre, P.B., Gessner, M.O., Dudgeon, D., Prusevich, A., Green, P., Glidden, S., Bunn, S.E., Sullivan, C.A., Liermann, C.R., Davies, P.M., 2010. Global threats to human water security and river biodiversity. Nature 467, 555–561. https://doi.org/10.1038/nature09440.

Vörösmarty, C.J., Meybeck, M., Fekete, B., Sharma, K., Green, P., Syvitski, J.P.M., 2003. Anthropogenic sediment retention: major global impact from registered river impoundments. Global Planet. Change 39, 169–190. https://doi.org/10.1016/S0921-8181(03)00023-7.

Ward, J.V., Stanford, J.A., 1983. Serial discontinuity concept of lotic ecosystems. Dyn. Lotic Syst. Ann Arbor Sci. Ann Arbor 29–42. https://doi.org/10.1016/j.ecolmodel.2009.06.022.

Webster, J.R., Benfield, E.F., Golladay, S.W., Hill, B.H., Hornick, L.E., Kazmierczak, R.F., Perry, W.B., 1987. Experimental studies of physical factors affecting seston transport in streams. Limnol. Oceanogr. 32, 848–863. https://doi.org/10.4319/lo.1987.32.4.0848.

Winemiller, K.O., McIntyre, P.B., Castello, L., Fluet-Chouinard, E., Giarrizzo, T., Nam, S., Baird, I.G., Darwall, W., Lujan, N.K., Harrison, I., Stiassny, M.L.J., Silvano, R.A.M., Fitzgerald, D.B., Pelicice, F.M., Agostinho, A.A., Gomes, L.C., Albert, J.S., Baran, E., Petrere, M., Zarfl, C., Mulligan, M., Sullivan, J.P., Arantes, C.C., Sousa, L.M., Koning, A.A., Hoeinghaus, D.J., Sabaj, M., Lundberg, J.G., Armbruster, J., Thieme, M.L., Petry, P., Zuanon, J., Torrente Vilara, G., Snoeks, J., Ou, C., Rainboth, W., Pavanelli, C.S., Akama, A., Van Soesbergen, A., Sáenz, L., 2016. Balancing hydropower and biodiversity in the amazon, Congo, and mekong. Science 84 351, 128–129. https://doi.org/10.1126/science.aac7082.

Wohl, E., Bledsoe, B.P., Jacobson, R.B., Poff, N.L., Rathburn, S.L., Walters, D.M., Wilcox, A.C., 2015. The natural sediment regime in rivers: broadening the foundation for ecosystem management. Bioscience 65, 358–371. https://doi.org/10.1093/biosci/biv002.

Yarnell, S.M., Petts, G.E., Schmidt, J.C., Whipple, A.A., Beller, E.E., Dahm, C.N., Goodwin, P., Viers, J.H., 2015. Functional flows in modified riverscapes: hydrographs, habitats and opportunities. Bioscience 65, 963–972. https://doi.org/10.1093/biosci/biv102.

Zarfl, C., Lumsdon, A.E., Berlekamp, J., Tydecks, L., Tockner, K., 2015. A global boom in hydropower dam construction. Aquat. Sci. 77, 161–170. https://doi.org/10.1007/s00027-014-0377-0.

Zolezzi, G., Siviglia, A., Toffolon, M., Maiolini, B., 2011. Thermopeaking in Alpine streams: event characterization and time scales. Ecohydrology 4, 564–576. https://doi.org/10.1002/eco.132.